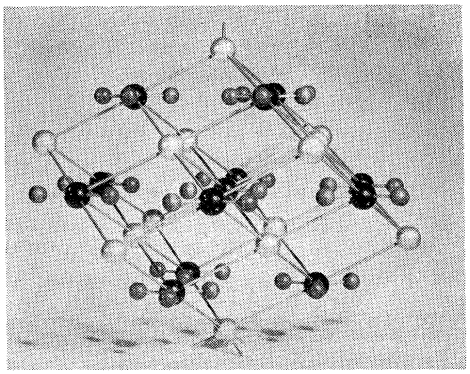

FIG. 10. Lattice structure of calcite.

concentration of color centers at highest coloration, computed by Smakula's formula,[19] is of the order $10^{16}/cm^3$. If we assume that some defects may be created by irradiation, the defects originally present must be less than $10^{-6}/cm^3$. The efficiency of coloration is given in Table I.

At low coloration levels about 300 ev are required to form one color center. This is of the same order as in calcium fluoride.[20] The efficiency of coloration decreases rapidly with irradiation dose similar to other crystals.

The strong luminescence with an emission band at 590 mμ can be considered as the recombination of the trapped electron with the hole and simultaneous decrease of the absorption bands. This process (the reverse of coloration) depends on temperature. Illumination with light of a wavelength exceeding 280 mμ did not produce any noticeable effect on bleaching or luminescence, nor could a photocurrent ($>10^{-12}$ amp) be observed.

[19] A. Smakula, Z. Physik **59**, 603 (1930).

[20] A. Smakula, Z. Physik **138**, 281 (1954).

PHYSICAL REVIEW VOLUME 124, NUMBER 6 DECEMBER 15, 1961

Diagrammatic Expansion for the Ising Model with Arbitrary Spin and Range of Interaction*

GERALD HORWITZ† AND HERBERT B. CALLEN
Department of Physics and Laboratory for Research on the Structure of Matter, University of Pennsylvania, Philadelphia, Pennsylvania

(Received March 23, 1961)

A new and simple diagrammatic expansion is developed for the free energy of the Ising model with arbitrary spin and range of interaction. The contribution of each diagram is a product of (1) the reciprocal of the order of the symmetry group of the diagram, (2) a product of semi-invariants, with a factor M_n for each spin in the diagram (n being the number of bonds joined to that spin) and (3) a sum of products $\Sigma_{i,j,k,\ldots}(2\beta J_{ij})(2\beta J_{kl})\cdots$, where $2\beta J_{ij}$ corresponds to a bond between spins i and j, and where the summation is carried out with no restrictions on the summation indices (i.e., no "excluded volume" corrections). The expansion variables are the spin deviation operators $\sigma_i \equiv \bar{S} - S_{iz}$. The quantity $\bar{S}$ is chosen to eliminate a large class of diagrams; this choice also minimizes the corresponding free-energy contribution and implies $\bar{S} = \langle S_{iz} \rangle$. By further renormalization of the vertices all reducible (i.e., simply articulated) diagrams are eliminated. To zero order the molecular field solution is obtained. The next approximation consists of the summation of renormalized simple loop diagrams. The justification of this choice of diagrams rests, at low temperature, on the decrease of the value of the higher order semi-invariants, on the relationship of these loop diagrams to the random phase approximation, and on the agreement with the rigorous low-temperature series result. At the Curie temperature the same choice of diagrams is justified by a modification of Brout's $1/z$ criterion, so that the expansion can be viewed as an expansion in $1/z$, where z is the effective number of spins interacting with a given spin. Finally the choice of loop diagrams is justified at high temperature by exact agreement to second order in T_c/T (and by a very close agreement to fourth order) with the rigorous high-temperature series expansion. Thus the theory agrees with rigorous results in the low-temperature and paramagnetic regions and has a well-defined criterion of validity in the intermediate temperature region. For nearest-neighbor interactions and spin $\frac{1}{2}$ the specific heat is continuous through the Curie temperature, with an infinite slope on the low-temperature side of the transition.

INTRODUCTION

THE Ising problem has been one of the most actively studied problems in statistical mechanics, principally due to its being perhaps the simplest model exhibiting a cooperative phenomenon, or phase transition.[1] In its simplest form, the spin-$\frac{1}{2}$ Ising model with nearest-neighbor interactions, it serves as a useful model for several physical systems, such as the ordering of binary alloys. Of particular interest to us is the fact that the Ising Hamiltonian is part of the ferromagnetic Heisenberg Hamiltonian, and that the Ising problem is a convenient preliminary to the ferromagnetic problem;

* Supported by the Office of Naval Research.

† Philco Fellow during part of this work.

[1] General references: G. F. Newell and E. Montroll, Revs. Modern Phys. **25**, 353 (1953). C. Domb, *Advances in Physics*, edited by N. F. Mott (Taylor and Francis, Ltd., London, 1960), Vol. 9, p. 140. H. N. V. Temperley, *Changes of State* (Cleaver-Hume, London, 1956), especially pp. 114–172. T. L. Hill, *Statistical Mechanics* (McGraw-Hill Book Company, New York, 1956), pp. 286–353.

we shall give the extension of the present methods to the ferromagnetic case in a subsequent paper. We here consider the Ising model of a ferromagnet with arbitrary spin, and with a strength of interaction ("exchange integral") which is an arbitrary function of the distance between the interacting spins.

Rigorous solutions have been given for the simple Ising model for one-dimensional and certain two-dimensional lattices.[2] There also exist series expansions which are valid for temperatures either very low[3] or very high[4] compared to the transition temperature T_c. Interpolations[1,5] between these regions provide the best available estimates of the Curie temperatures (or transition temperatures) of three-dimensional lattices.

A number of heuristically appealing approximate methods have been proposed, such as the molecular field (or Bragg-Williams) method,[6] the Bethe-Peierls method,[7] the Kikuchi method,[8] and others. Most of these are in some sense an extension of the molecular field method, treating a small cluster of spins accurately and representing the remainder of the system in terms of its average properties.

In the limit of an infinite range of interaction, in which each spin interacts equally with every other spin in the lattice, the molecular field method becomes rigorous, and all the cluster methods merge.

The heuristic cluster methods have the advantage of providing closed form solutions and of having solutions through the transition region. Their disadvantage is their lack of a criterion of validity, or of a well-defined procedure for successively higher approximation; that is, they do not generally possess clear-cut expansion parameters.

Another important approximation is afforded by the spherical model,[9] obtained from the Ising model by relaxing certain mathematical constraints. In particular, the spherical model permits each spin to be of arbitrary magnitude, constraining only the sum of the squares of all the spin magnitudes to have the proper prescribed value. Solution of this model, which can be carried out rigorously, gives a Curie temperature somewhat below the best estimates for the Ising model. It predicts a specific heat continuous at the Curie temperature, but with infinite slope on both high- and low-temperature sides of the transition. As we shall see, the results of our first-order approximation give a Curie temperature very close to that of a spherical model. The specific heat is again continuous, but has an infinite slope only on the low-temperature side of the transition.

A form of expansion was developed by Kirkwood,[10] which, although it did not prove to be convenient, furnished a point of departure for a recent work by Brout.[11] Kirkwood's method used the formalism of semi-invariants to effect an expansion in powers of $1/kT$, valid at high temperatures. He utilized an ensemble microcanonical with respect to the z component of the total spin, thereafter evaluating the z component of spin to minimize the resultant free energy. Brout extended this analysis by rearranging the terms in the Kirkwood expansion, abandoning the criterion of expansion in powers of $1/kT$. Instead, he classified and ordered the terms in the Kirkwood expansion in powers of the expansion parameter $1/z$. Here z is the effective number of spins interacting with a given spin—a number of the order of 8 to 12 even for nearest-neighbor interactions, and larger for a system with long-range interactions. If every spin interacts with every other spin ($z\rightarrow\infty$) the molecular field method becomes rigorous, so that the molecular field result is the leading order term in Brout's expansion. Brout refers to the $1/z$ expansion as a "high-density expansion."

The approach which we develop in this paper has many similarities to Brout's method, but there are a number of fundamental differences. Firstly, we use a canonical formalism with respect to the z component of spin, rather than Kirkwood's microcanonical formalism. Secondly, our treatment applies to arbitrary spin rather than being limited to the case of spin $\frac{1}{2}$. Thirdly, we regroup the semi-invariant terms of the Kirkwood series into new basic terms which obviate the need for restrictions on the summation indices; these restrictions were responsible for Brout's "dotted-line diagrams" and for a considerable complexity in his treatment.

The expansion variables in terms of which our theory is formulated are the spin deviation operators $\sigma_i=\bar{S}-S_{iz}$. The quantity $\bar{S}$ is chosen to eliminate a large class of diagrams; this choice also minimizes the corresponding free-energy contribution and implies the self-consistency relation $\bar{S}=\langle S_{iz}\rangle$. By further renormalization of the vertices we eliminate all reducible diagrams (defined as linked diagrams which can be separated into unlinked parts by a single cut). Thus the renormalized diagrams actually represent many unrenormalized diagrams, and the diagrams which are summed represent relatively large fractions of the over-all interaction. The renormalization procedure establishes an irreducible linked diagram expansion for the Ising model.

The zero-order approximation in the theory yields the internal field or Bragg-Williams result. The first approximation consists of the summation of all simple

[2] L. Onsager, Phys. Rev. **65**, 117 (1944). B. Kaufman, Phys. Rev. **76**, 1232 (1949). M. Kac and J. C. Ward, Phys. Rev. **88**, 1332 (1952).
[3] C. Domb and M. F. Sykes, Proc. Roy. Soc. (London) **A235**, 247 (1956).
[4] A. J. Wakefield, Proc. Cambridge Phil. Soc. **47**, 419 (1951). G. S. Rushbrooke and I. Scoins, Proc. Roy. Soc. (London) **A230**, 74 (1955). C. Domb and M. F. Sykes, Proc. Roy. Soc. (London) **A240**, 214 (1957).
[5] E. Trefftz, Z. Physik **127**, 371 (1950).
[6] W. L. Bragg and E. J. Williams, Proc. Roy. Soc. (London) **A145**, 699 (1934); **A151**, 540 (1935).
[7] H. A. Bethe, Proc. Roy. Soc. (London) **A150**, 552 (1935). R. Peierls, Proc. Cambridge Phil. Soc. **32**, 471 (1936); Proc. Roy. Soc. (London) **A154**, 207 (1936).
[8] R. Kikuchi, Phys. Rev. **81**, 988 (1951).
[9] T. Berlin and M. Kac, Phys. Rev. **86**, 821 (1952); M. Lax, *ibid.* **97**, 629 (1955).
[10] J. G. Kirkwood, J. Chem. Phys. **6**, 70 (1938).
[11] R. Brout, Phys. Rev. **115**, 824 (1959); **118**, 1009 (1960).

renormalized loop diagrams, the second approximation consists of the summation of all double-loop renormalized diagrams, etc. We carry out the calculation explicitly to the first order.

The justification of the above classification of diagrams, in our opinion, cannot be based on a single consideration valid for all temperature ranges. However, we believe that there are sufficient evidences of the validity of the procedure to indicate that the method is a valid procedure for all temperature regions. The fact that the free energy is minimum with respect to $\bar{S}$ at each stage of the approximation is one important guide to the ordering of diagrams; this criterion is not satisfied if, for instance, the unrenormalized simple loop diagrams alone are summed. At very low temperatures the first-order theory agrees with the rigorous low-temperature series result—furthermore, the higher-order diagrams involve higher-order semi-invariants, which we expect to fall off rapidly in value. At high temperatures[12] the results agree with the rigorous expansion in inverse powers of the temperature exactly to second power in $1/T$ and to an excellent approximation to $1/T^4$. In the vicinity of the Curie temperature, the classification of diagrams corresponds to an expansion in powers of $1/z$, where z is the effective number of spins interacting with a given spin. The application of the $1/z$ classification to the renormalized diagrams thereby modifies Brout's criterion in a fundamental fashion, which we show to be at least self-consistent. Thus, by all the above considerations, and by the agreement of our results with the rigorous results in the regions of the latter's validity, we believe that the ordering of the renormalized diagrams according to their numbers of loops defines a valid and convergent approximation scheme at all temperatures.

In Sec. 1, the Hamiltonian is written in terms of the spin deviation operators and is separated into the noninteracting ("unperturbed") part and the interacting ("perturbation") portion. The corresponding contributions to the free energy are computed, and the unperturbed free energy is shown to correspond to a molecular field result, with a molecular field proportional to $\bar{S}$. In Sec. 2 the properties of semi-invariants are analyzed. The linked cluster expansion of the free energy is set up and characterized by a diagram convention in Sec. 3. In Sec. 4 we regroup the terms of the linked cluster expansion into the more convenient type of series referred to previously, and a new diagram convention is introduced to characterize the terms of this new series. A more detailed analysis of the rearrangement of the expansion, and an analysis of the resultant series, is given in Sec. 5. Section 6 briefly recapitulates Brout's $1/z$ classification of diagrams. The simplest form of renormalization of $\bar{S}$ is presented in Sec. 7, eliminating zero-order diagrams ("Cayley trees") and establishing the simple molecular field result. The renormalization procedure required for this purpose does not eliminate all reducible diagrams, and we show in Sec. 8 that it is not a satisfactory procedure for the higher orders. In particular, the simple renormalization procedure leaves certain reducible diagrams in first order; these are directly summed and are shown to lead to a formal divergence of the magnetization at the Curie temperature. Having thus demonstrated the necessity of a fully self-consistent renormalization, we analyze one aspect of renormalization procedures in Sec. 9.

In particular, we show that certain large classes of diagrams can be eliminated by appropriate choice of $\bar{S}$, and that this choice both minimizes the free energy and evaluates $\bar{S}$ self-consistently as the magnetization. The basis for this choice of $\bar{S}$ is developed in Appendixes A and B, and the fact that it is not yet a sufficient renormalization is shown in Appendix C. The second aspect of a full renormalization procedure, eliminating all remaining reducible diagrams ("Husimi trees"), is also briefly described in Sec. 9 and is illustrated in detail in Sec. 10, in which the free energy is explicitly calculated to first order by summation of the simple renormalized loops. Finally, the results are computed and discussed in Sec. 11.

The Curie temperatures of several simple lattices, with nearest-neighbor interactions and spin $\frac{1}{2}$, are compared with the results of several other investigations in Table I. The Curie temperatures are somewhat lower than the results of most other analytic theories, but are in close agreement with the results of the spherical model and with the estimates made by Trefftz[5] on the basis of graphical extrapolation of the reciprocal specific heats obtained from exact series expansions at high and low temperatures. To first order the specific heat is found to be continuous at T_c, with an infinite slope on the low-temperature side of the transition but (in contrast with the spherical model) with a finite slope on the high-temperature side.

1. THE HAMILTONIAN

We consider a crystal containing N equivalent lattice sites, each occupied by a spin S. The spins interact by an Ising interaction $(-J_{ij}S_{iz}S_{jz})$ with a positive "exchange integral" J_{ij}. The exchange integral is not restricted to nearest neighbors, but is assumed to be a function of the distance between the interacting spins only. With an applied field along the negative z axis, the Hamiltonian is

$$\mathcal{H}=-\sum_{i,j} J_{ij}S_{iz}S_{jz}-g\mu_0 H\sum_i S_{iz}. \tag{1}$$

The first summation extends over all i and j, and we define J_{ii} as zero. The quantity g is the Landé factor, μ_0 is the Bohr magneton, and H is the magnetic field;

[12] Extension of the method would easily give rigorous coefficients for the higher order terms in $1/T$, and would provide a very convenient alternative to the very laborious method of obtaining the high-temperature expansion by the Kirkwood method.

the quantity $g\mu_0 H$ is positive and all spins have $S_z=+S$ in the ground state.

We introduce the spin deviation operator

$$\sigma_i=\bar{S}-S_{iz}, \tag{2}$$

where $\bar{S}$ is a quantity to be chosen subsequently. The Hamiltonian becomes

$$\mathcal{H}=\mathcal{H}_0+V, \tag{3}$$

where

$$\mathcal{H}_0=E_0+L\sum_i \sigma_i, \tag{4}$$

$$E_0=-N\bar{S}(g\mu_0 H+J_0\bar{S}), \tag{5}$$

$$J_0=\sum_j J_{ij} \quad \text{(a quantity independent of } i\text{)}, \tag{6}$$

$$L=g\mu_0 H+2J_0\bar{S}, \tag{7}$$

and

$$V=-\sum_{i,j} J_{ij}\sigma_i\sigma_j. \tag{8}$$

The "unperturbed" Hamiltonian H_0 is a sum of single-spin operators and the quantity $L/g\mu_0$ can be considered as an effective magnetic field acting on the spin deviations.

The magnetic Gibbs function, or "free energy," is given by

$$-\beta F=\ln \operatorname{tr}\exp[-\beta(\mathcal{H}_0+V)], \tag{9}$$

where $\beta=1/kT$, and where the Hamiltonian H_0 is actually the magnetic Hamiltonian (already transformed with respect to the external field) as defined by Eqs. (4)–(7). Thus, F is a thermodynamic function of T and H, the analog of the Gibbs function (which depends on T and pressure).

Separating off the contribution to F arising from H_0 alone, we write

$$-\beta F=-\beta F_0-\beta F', \tag{10}$$

where

$$-\beta F_0=\ln \operatorname{tr}\exp(-\beta\mathcal{H}_0), \tag{11}$$

and

$$-\beta F'=\ln \operatorname{tr}\left[\exp(-\beta V)\frac{\exp(-\beta\mathcal{H}_0)}{\operatorname{tr}\exp(-\beta\mathcal{H}_0)}\right]. \tag{12}$$

The quantity F_0 can be evaluated easily in the representation in which each of the σ_i is diagonal:

$$-\beta F_0=\ln \operatorname{tr}\exp[-\beta(E_0+L\textstyle\sum_i \sigma_i)] \tag{13}$$

$$=-\beta E_0-\beta NL\bar{S}+N\ln\sum_{-S}^{S}\exp(\beta LS_z) \tag{14}$$

$$=-\beta NJ_0\bar{S}^2+N\ln\sum_{-S}^{S}\exp(\beta LS_z) \tag{15}$$

$$=-\beta NJ_0\bar{S}^2+N\ln\sinh[\beta L(S+\tfrac{1}{2})]-N\ln\sinh(\tfrac{1}{2}\beta L). \tag{16}$$

The remaining term in the free energy F' can be written formally as an average by introducing the weighting factor ρ,

$$\rho=\frac{\exp(-\beta\mathcal{H}_0)}{\operatorname{tr}\exp(-\beta\mathcal{H}_0)}=\prod_i \rho_i, \tag{17}$$

where the single-spin weighting factor ρ_i is

$$\rho_i=\exp(-\beta L\sigma_i)/\sum_{\bar{S}-S}^{\bar{S}+S}\exp(-\beta L\sigma_i)=\exp(\beta LS_{iz})/\sum_{-S}^{S}\exp(\beta LS_{iz}). \tag{18}$$

Then, using the notation $\langle\ \rangle$ to denote an average with respect to the weighting factor ρ, we rewrite Eq. (12) in the form

$$-\beta F'=\ln \operatorname{tr}(\rho e^{-\beta V})=\ln\langle e^{-\beta V}\rangle. \tag{19}$$

2. SEMI-INVARIANTS, OR CUMULANTS

Preparatory to our expansion of F', we consider a quantity of the form

$$\phi(a)=\ln\langle e^{ax}\rangle=\ln \operatorname{tr}[e^{ax}\rho(x)], \tag{20}$$

where a is a constant and $\rho(x)$ is a normalized weighting factor. Such quantities arise frequently in statistical theory; when expanded in powers of a the coefficients define the so-called semi-invariants or cumulants $M_n(x)$:

$$\phi(a)=\sum_{n=1}^{\infty}\frac{a^n}{n!}M_n(x). \tag{21}$$

It is, of course, clear that $M_n(x)$ is not a function of x, but is simply a constant; the functional notation $M_n(x)$ merely identifies the variable x with respect to which M_n is defined. A useful symbolic way of carrying out the expansion provides a convenient closed expression for the semi-invariants. We rewrite Eq. (20) in the form

$$\phi(a)=\lim_{\alpha\to 0}\ln\langle e^{ax}\rangle_\alpha=\lim_{\alpha\to 0}\ln \operatorname{tr}[e^{ax}\rho_\alpha(x)], \tag{22}$$

where

$$\rho_\alpha(x)=e^{\alpha x}\rho(x). \tag{23}$$

Hence,

$$\phi(a)=\lim_{\alpha\to 0}\ln \operatorname{tr}[e^{(a+\alpha)x}\rho(x)] \tag{24}$$

$$=\lim_{\alpha\to 0}e^{aD_\alpha}\ln \operatorname{tr}[e^{\alpha x}\rho(x)], \tag{25}$$

where

$$D_\alpha=\partial/\partial\alpha, \tag{26}$$

and where e^{aD_α} is the translation operator which transforms a function of α to the same function of $(a+\alpha)$. Expanding e^{aD_α} in power series,

$$\phi(a)=\lim_{\alpha\to 0}\sum_{n=0}^{\infty}\frac{a^n}{n!}D_\alpha{}^n\ln \operatorname{tr}[e^{\alpha x}\rho(x)], \tag{27}$$

and noting that the $n=0$ term vanishes by the normalization of ρ, we find

$$\phi(a)=\lim_{\alpha\to 0}\sum_{n=1}^{\infty}\frac{a^n}{n!}D_\alpha{}^n \ln \mathrm{tr}[e^{\alpha x}\rho(x)]. \tag{28}$$

Comparing Eqs. (28) and (21) we identify the semi-invariants

$$M_n(x)=\lim_{\alpha\to 0}M_n{}^{(\alpha)}(x), \tag{29}$$

$$M_n{}^{(\alpha)}(x)=D_\alpha{}^n \ln \mathrm{tr}[e^{\alpha x}\rho(x)]. \tag{30}$$

Or, noting that $D_\alpha \ln \mathrm{tr}[e^{\alpha x}\rho(x)]$ is simply $\langle x\rangle_\alpha$, Eq. (30) can be rewritten

$$M_n{}^{(\alpha)}(x)=D_\alpha{}^{n-1}\langle x\rangle_\alpha=D_\alpha M_{n-1}{}^{(\alpha)}(x). \tag{31}$$

Equation (31) can be used to compute the semi-invariants directly, but the following identity is useful for this purpose

$$D_\alpha\langle x^n\rangle_\alpha=D_\alpha\frac{\mathrm{tr}(x^n e^{\alpha x}\rho)}{\mathrm{tr}(e^{\alpha x}\rho)}=\langle x^{n+1}\rangle_\alpha-\langle x^n\rangle_\alpha\langle x\rangle_\alpha. \tag{32}$$

With these two equations [(31) and (32)] we now find easily that

$$M_1{}^{(\alpha)}(x)=\langle x\rangle_\alpha, \tag{33}$$

$$M_2{}^{(\alpha)}(x)=\langle x^2\rangle_\alpha-\langle x\rangle_\alpha{}^2, \tag{34}$$

$$M_3{}^{(\alpha)}(x)=\langle x^3\rangle_\alpha-3\langle x^2\rangle_\alpha\langle x\rangle_\alpha+2\langle x\rangle_\alpha{}^3, \tag{35}$$

$$M_4{}^{(\alpha)}(x)=\langle x^4\rangle_\alpha-4\langle x^3\rangle_\alpha\langle x\rangle_\alpha-3\langle x^2\rangle_\alpha +12\langle x^2\rangle_\alpha\langle x\rangle_\alpha{}^2-6\langle x\rangle_\alpha{}^4. \tag{36}$$

In the following we retain the symbol α explicitly only when necessary for clarity. The appearance of the D operator in any equation implies first that ρ is to be replaced by ρ_α and that finally the limit $\alpha\to 0$ is to be taken. It should be noted that since ρ_α is not normalized, replacing ρ by ρ_α requires that the appropriate normalization denominators be introduced. Thus $\langle x^n\rangle = \mathrm{tr}\, x^n\rho$ but $\langle x^n\rangle_\alpha=\mathrm{tr}\, x^n\rho_\alpha/\mathrm{tr}\rho_\alpha$.

The semi-invariants clearly satisfy the following identities:

$$M_n(bx)=b^nM_n(x), \tag{37}$$

$$M_n(x+b)=M_n(x) \quad \text{if} \quad n>1, \tag{38}$$

$$M_1(x+b)=M_1(x)+b. \tag{39}$$

Another closed form expression for the nth semi-invariant is

$$M_n(x)=-n!\sum_{\{p_j\}}\left\{[\sum_i(p_j-1)!]\prod_i\frac{(-1)^{p_j}\langle x^j\rangle^{p_j}}{p_j!(j!)^{p_j}}\right\}, \tag{40}$$

where the first summation is over all sets of non-negative integers $p_1, p_2\cdots p_n$ such that

$$\sum_{j=1}^{n}jp_j=n. \tag{41}$$

We note that the identity (32) also provides a useful operator for expressing the moments $\langle x^n\rangle$ in terms of the semi-invariants, for we can rewrite that equation in the form

$$[D+\langle x\rangle]\langle x^n\rangle=\langle x^{n+1}\rangle, \tag{42}$$

or

$$\langle x^n\rangle=[D+\langle x\rangle]^{n-1}\langle x\rangle. \tag{43}$$

and therefore,

$$\langle x^n\rangle=[D+M_1(x)]^{n-1}M_1(x)=[D+M_1(x)]\langle x^{n+1}\rangle. \tag{44}$$

In particular, we obtain

$$\langle x^2\rangle=[D+M_1]M_1=M_2+M_1{}^2, \tag{45}$$

$$\langle x^3\rangle=[D+M_1](M_2+M_1{}^2) \tag{46}$$

$$=M_3+3M_1M_2+M_1{}^3, \tag{47}$$

and this process of step-wise generation of higher moments is very easily continued.

3. LINKED CLUSTER EXPANSION OF $-\beta F'$

Recalling that

$$-\beta F'=\ln\langle e^{-\beta V}\rangle, \tag{48}$$

we expand in powers of β, as in Eq. (21), obtaining

$$-\beta F'=\sum_{n=1}^{\infty}\frac{\beta^n}{n!}M_n(-V), \tag{49}$$

where, as in Eqs. (29) and (30),

$$M_n(-V)=\lim_{\alpha\to 0}M_n{}^{(\alpha)}(-V)=\lim_{\alpha\to 0}D_\alpha{}^{n-1}\langle -V\rangle_\alpha =\lim_{\alpha\to 0}D_\alpha{}^n \ln \mathrm{tr}(e^{-\alpha V}\rho). \tag{50}$$

We now wish to consider the fact that V is the sum of terms corresponding to all pairs of spins in the lattice:

$$-V=\sum_{i,j}J_{ij}\sigma_i\sigma_j=\sum_{(i,j)}2J_{ij}\sigma_i\sigma_j, \tag{51}$$

where (i,j) denotes summation over all *pairs* of indices i and j. To investigate the consequences of this form of V we define a set of parameters α_{ij} which will replace the single parameter α. In place of ρ_α we define $\rho_{\{\alpha\}}$ by the equation

$$\rho_{\{\alpha\}}=\rho\exp\sum_{(i,j)}\alpha_{ij}\sigma_i\sigma_j=\rho\prod_{(i,j)}e^{\alpha_{ij}\sigma_i\sigma_j}, \tag{52}$$

and

$$\langle -V\rangle_{\{\alpha\}}=\frac{\mathrm{tr}(-V\rho_{\{\alpha\}})}{\mathrm{tr}\rho_{\{\alpha\}}}=\sum_{(i,j)}2J_{ij}\langle\sigma_i\sigma_j\rangle_{\{\alpha\}}. \tag{53}$$

The derivative D_α is now replaced by

$$D_{\{\alpha\}}=\sum_{(i,j)}2J_{ij}\frac{\partial}{\partial\alpha_{ij}}=\sum_{(i,j)}2J_{ij}D_{ij}. \tag{54}$$

Then

$$M_n(-V)=\lim_{\{\alpha\}\to 0} M_n^{\{\alpha\}}(-V)$$
$$=\lim_{\{\alpha\}\to 0}\Big(\sum_{(i,j)} 2J_{ij}D_{ij}\Big)^n \ln \mathrm{tr}\rho_{\{\alpha\}}. \quad (55)$$

Expanding the quantity $(\sum_{(i,j)} 2J_{ij}D_{ij})^n$ by the multinomial expansion, we write

$$\Big(\sum_{(i,j)} 2J_{ij}D_{ij}\Big)^n = n!\sum_{\{p_{ij}\}}\prod_{(ij)}\frac{(2J_{ij})^{p_{ij}}}{p_{ij}!}D_{ij}^{p_{ij}}, \quad (56)$$

where the summation is over all sets of non-negative integers p_{ij} satisfying the equality

$$\sum_{(i,j)} p_{ij}=n. \quad (57)$$

Thus

$$-\beta F'=\lim_{\{\alpha\}\to 0}\sum_{\{p_{ij}\}}\prod_{(i,j)}\frac{1}{p_{ij}!}(2\beta J_{ij}D_{ij})^{p_{ij}} \ln \mathrm{tr}\rho_{\{\alpha\}}, \quad (58)$$

where $\prod_{(ij)}\beta^{p_{ij}}=\beta^n$, and where the summation over n in Eq. (49) is effected in Eq. (58) merely by removing the restriction (57) on the summation of the p_{ij}.

Consider the result of operating with D_{ij}:

$$D_{ij}\ln \mathrm{tr}\rho=\lim_{\{\alpha\}\to 0} D_{ij}\ln \mathrm{tr}\rho_{\{\alpha\}}=\langle\sigma_i\sigma_j\rangle, \quad (59)$$

and

$$D_{kl}D_{ij}\ln \mathrm{tr}\rho=D_{kl}\langle\sigma_i\sigma_j\rangle=\langle\sigma_i\sigma_j\sigma_k\sigma_l\rangle-\langle\sigma_i\sigma_j\rangle\langle\sigma_k\sigma_l\rangle, \quad (60)$$

where we have omitted the notation $\{\alpha\}$ and where the limiting process is again understood. Similarly,

$$D_{ij}\langle\phi\rangle=\langle\phi\sigma_i\sigma_j\rangle-\langle\phi\rangle\langle\sigma_i\sigma_j\rangle \quad (61)$$

in analogy with Eq. (32). In this way we generate the quantity $\prod_{(ij)} D_{ij}^{p_{ij}}\ln \mathrm{tr}\rho_{\{\alpha\}}$ in complete analogy with the manner in which a semi-invariant is generated [Eq. (31)]. For a given set of integers $\{p_{ij}\}$ we define

$$M_{\{p_{ij}\}}=\prod_{(ij)} D_{ij}^{p_{ij}}\ln \mathrm{tr}\rho, \quad (62)$$

and $M_{\{p_{ij}\}}$ has precisely the form of $M_n(-V)$, but in each term there are p_{12} factors $\sigma_1\sigma_2$, p_{23} factors $\sigma_2\sigma_3$, $\cdots$ instead of n equal factors $(-V)$. Thus

$$M_{\{p_{ij}\}}=\langle\sigma_1\sigma_2\rangle \quad \text{if} \quad p_{12}=1 \quad \text{and all other} \quad p_{ij}=0, \quad (63)$$

$$M_{\{p_{ij}\}}=\langle\sigma_1\sigma_2\sigma_2\sigma_3\rangle-\langle\sigma_1\sigma_2\rangle\langle\sigma_2\sigma_3\rangle$$
$$\text{if} \quad p_{12}=p_{23}=1, \quad \text{all other} \quad p_{ij}=0, \quad (64)$$

$$M_{\{p_{ij}\}}=\langle(\sigma_1\sigma_2)^2\sigma_2\sigma_3\rangle-2\langle\sigma_1\sigma_2\rangle\langle\sigma_1\sigma_2\sigma_2\sigma_3\rangle$$
$$-\langle(\sigma_1\sigma_2)^2\rangle\langle\sigma_2\sigma_3\rangle+2\langle\sigma_1\sigma_2\rangle^2\langle\sigma_2\sigma_3\rangle$$
$$\text{if} \quad p_{12}=2, \quad p_{23}=1, \quad \text{other} \quad p_{ij}=0. \quad (65)$$

With this notation we now have

$$-\beta F'=\sum_{\{p_{ij}\}}\Big[\prod_{(ij)}\frac{1}{p_{ij}!}(2\beta J_{ij})^{p_{ij}}\Big]M_{\{p_{ij}\}}. \quad (66)$$

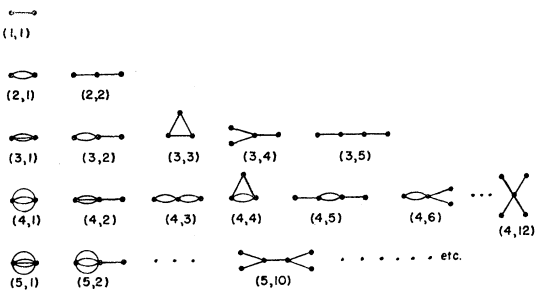

FIG. 1. Diagrammatic representation of terms.

Each term in this expansion, corresponding to a particular set of integers $\{p_{ij}\}$, can be represented by a diagram. To do so we simply draw p_{ij} bonds between i and j, for each integer p_{ij} in the set. To every choice of a set of integers there corresponds a diagram, and the contribution to $-\beta F'$ of that diagram is

$$\Big(\prod_{(i,j)}\frac{1}{p_{ij}!}(2\beta)^{p_{ij}}J_{ij}^{p_{ij}}\Big)M_{\{p_{ij}\}},$$

where p_{ij} is the multiplicity of the bonds connecting sites i and j.

We see immediately that the term corresponding to any choice of integers $\{p_{ij}\}$ vanishes if the nonzero integers p_{ij} can be divided into two sets with no indices in common. That is, all "unlinked diagrams" vanish. This follows from the fact that in generating $M_{\{p_{ij}\}}$ by Eq. (62) we can first apply all the D_{kl} in one set. When we then apply a D_{ij} from the second (nonoverlapping) set the quantity immediately vanishes. To see this we let $\langle\phi\rangle$ be one of the averages generated by the D_{kl} of the first set, so that ϕ involves the $\sigma_k\sigma_l$ in this set. We can let all the α_{ki} which join the two sets vanish, and $\rho_{\{\alpha\}}$ factors into $\rho_1\rho_2$, where ρ_1 involves the spins of the first set and ρ_2 involves the spins of the second set. Then

$$\langle\phi\rangle=\frac{\mathrm{tr}(\phi\rho_1\rho_2)}{\mathrm{tr}(\rho_1\rho_2)}=\frac{[\mathrm{tr}(\phi\rho_1)][\mathrm{tr}(\rho_2)]}{(\mathrm{tr}\rho_1)(\mathrm{tr}\rho_2)}=\frac{\mathrm{tr}(\phi\rho_1)}{\mathrm{tr}\rho_1},$$

and this quantity is independent of the indices of the second set. Hence $D_{ij}\langle\phi\rangle=0$, proving that all such unlinked diagrams vanish.

All diagrams [or terms in Eq. (66)] can be grouped into sets of "topologically equivalent diagrams." A set of topologically equivalent diagrams is defined by the requirement that every diagram of the set is carried into a diagram of the set by any one-to-one relabeling of the sites of the lattice. We denote such sets of diagrams by the two indices (n,t), where the integer n specifies the number of bonds in a diagram, and t then numbers the various topologically equivalent sets of diagrams with n bonds.

For $n=1$ there is only a single set, designated by (1,1), and consisting of a single bond, as shown in Fig. 1.

For $n=2$ there are two sets of topologically equivalent diagrams. One set, designated by (2,1), consists of double bonds. The second set (2,2) consists of pairs of connected single bonds, which again are indicated in Fig. 1.

For $n=3$ there are five sets: triple bonds, (3,1); connected double and single bonds, (3,2); triangles, (3,3); branched chains, (3,4); and chains of single bonds, (3,5).

It should be noted that the diagrams in a set are similar only in a topological sense—the angles between bonds and the lengths of the bonds are irrelevant to the classification.

Let us suppose that a particular set of integers $\{p_{ij}\}_{n,t}$ corresponds to a diagram in the set (n,t). The contribution of this diagram to $-\beta F'$ is

$$(2\beta)^n M_{\{p_{ij}\}} \prod_{(ij)} \left(\frac{1}{p_{ij}!}\right) \prod_{(ij)} J_{ij}^{p_{ij}}. \tag{67}$$

However the quantity $M_{\{p_{ij}\}}$ is independent of the particular indices selected; that is, it is the same for all diagrams in the topologically equivalent set. As a particular example, any diagram in the set (2,2) (consisting of two connected single bonds) has

$$M_{\{p_{ij}\}}=\langle\sigma_1\sigma_2\sigma_2\sigma_3\rangle-\langle\sigma_1\sigma_2\rangle\langle\sigma_2\sigma_3\rangle=\langle\sigma\rangle^2\langle\sigma^2\rangle-\langle\sigma\rangle^4.$$

We consequently designate $M_{\{p_{ij}\}}$ by $M_{(n,t)}$. Similarly, the product $\prod_{(ij)}(1/p_{ij}!)$ is the same for every diagram in a set; it is unity for the set of two connected single bonds, and it is $1/3!$ for the set of triple bonds. We denote this product by $P_{n,t}$.

The summation over all diagrams in Eq. (66) can be replaced by a two-step summation; first over all classes of diagrams and then over all diagrams within a class. Thus

$$-\beta F'=\sum_{n,t}(2\beta)^n M_{(n,t)} P_{n,t} \sum_{\{p_{ij}\}} \prod_{(ij)} J_{ij}^{p_{ij}}, \tag{68}$$

where the second summation is to be taken over all choices of integers $\{p_{ij}\}$ which give diagrams in the set (n,t). In this last summation the quantity to be summed is a product of n exchange integrals, with some indices repeating in a way which is characteristic of the class (n,t). Thus for the class of triangular three-bond diagrams the product to be summed is of the form $J_{ij}J_{jk}J_{ki}$. For the class of diagrams (3,2) the summand is of the form $J_{ij}^2 J_{jk}$.

We inquire as to the possibility of replacing the last summation in Eq. (68) by a simple summation over the indices. Thus for triangular diagrams we consider the summation $\sum_{i,j,k} J_{ij}J_{jk}J_{ki}$. Obviously, this latter sum reproduces all triangular diagrams, but it repeats every diagram six times. This sixfold repetition results from the fact that the product $J_{12}J_{23}J_{31}$, which should be counted once, occurs when $(i,j,k)=(1,2,3)$, $(3,1,2)$, $(2,3,1)$, $(3,2,1)$, $(1,3,2)$, or $(2,1,3)$. Hence the final summation in Eq. (68) can be replaced by $\frac{1}{6}\sum_{ijk} J_{ij}J_{jk}J_{ki}$.

Let $W_{n,t}$ be the number of ways in which the vertices of a diagram in the set (n,t) can be numbered $1, 2, 3\cdots$, keeping the connectivity of these indices unchanged—that is, if vertex 1 is bonded to vertex 2 in one numbering it must be in all numberings. Then the final summation in Eq. (68) can be replaced by $W_{n,t}^{-1}\sum_{i,j,k\ldots}{}'(\ )$ where the prime on the summation excludes overlapping values of the summation indices.

For the class of square diagrams we find $W_{n,t}=8$ and the summation in Eq. (68) can be replaced by

$$\tfrac{1}{8}\sum_{i,j,k,l}{}' J_{ij}J_{jk}J_{kl}J_{li},$$

where the prime on the summation implies $i\neq k$ and $j\neq l$. It is, of course, immaterial whether $i=j$, etc., as $J_{ii}=0$.

Similarly, for the diagrams (3,2) we find $W_{n,t}=1$, whereas for (5,10) we find $W_{n,t}=8$.

It is convenient to write $P_{n,t}W_{n,t}^{-1}=G_{n,t}^{-1}$, so that $G_{n,t}$ is the product of $W_{n,t}$ and the factorials of the multiplicities of each of the bonds in the diagrams. Then we can rewrite Eq. (68) in the form

$$-\beta F'=\sum_{n,t}(2\beta)^n M_{(n,t)} G_{n,t}^{-1} \sum_{i,j\cdots}{}' J_{ij}J_{jk}\cdots, \tag{69}$$

where the pattern of repetitions of the indices in the final summand corresponds to the class (n,t) of topologically equivalent diagrams.

A convenient interpretation of the quantity $G_{n,t}$ is in terms of the order of the symmetry group of the diagram (n,t). The symmetry operations permitted are permutations of equivalent parts of the diagrams. Thus for the diagram (5,10) we can reflect the entire diagram through a vertical line, or we can reflect either the left-hand fork or the right-hand fork through a horizontal line, thereby permuting or interchanging the equivalent arms of the fork. Each of these operations is a twofold operation, giving $G_{n,t}=2\times2\times2=8$. If the central bond were a double bond, $G_{n,t}$ would contain an additional factor of two.

For multiple bonds the symmetry group contains the $p!$ permutation operations, where p is the bond multiplicity.

The linked cluster expansion, Eq. (69), is essentially that obtained by Brout.[11] We are concerned with this form of expansion only as an intermediate step, proceeding to a further rearrangement of Eq. (69) to obtain a series in which the terms have a simpler form, and in which the troublesome restrictions on the indices (indicated by the prime on the last summation) are removed.

4. REARRANGEMENT OF THE CLUSTER EXPANSION

In the next section we will rearrange the terms in the linked cluster expansion to introduce a new type of expansion. In this section we first demonstrate this

rearrangement for the particular cases of one-, two-, and three-bond diagrams.

For the class of single bonds we have

$$-\beta F_{(1,1)}=2\beta\langle\sigma_1\sigma_2\rangle\tfrac{1}{2}\sum_{i,j}J_{ij}=\tfrac{1}{2}N(2\beta)J_0M_1^2, \quad (70)$$

where $M_1=\langle\sigma\rangle$ and where the factor of $\frac{1}{2}$ arises from the factor $G_{1,1}^{-1}$. The quantity J_0 was previously defined [Eq. (6)]. In this case the terms are of simple form and require no rearrangement.

For the class of two connected single bonds we have

$$-\beta F_{(2,2)}=(2\beta)^2[\langle\sigma_1\sigma_2^2\sigma_3\rangle-\langle\sigma_1\sigma_2\rangle\langle\sigma_2\sigma_3\rangle]\tfrac{1}{2}\sum_{i,j,k}{}'J_{ij}J_{jk}$$
$$=\tfrac{1}{2}(2\beta)^2M_1M_2M_1\sum_{ijk}{}'J_{ij}J_{jk}. \quad (71)$$

The remaining class of two-bond diagrams is the class of double bonds. For these, $G_{2,1}=4$, corresponding to the interchange of bonds and to the reflection operation which interchanges the vertices. Hence

$$-\beta F_{(2,1)}=(2\beta)^2[\langle\sigma_1^2\sigma_2^2\rangle-\langle\sigma_1\sigma_2\rangle^2]\tfrac{1}{4}\sum_{ij}J_{ij}^2$$
$$=(2\beta)^2[(M_2+M_1^2)^2-M_1^4]\tfrac{1}{4}\sum_{i,j}J_{ij}^2$$
$$=\tfrac{1}{4}(2\beta)^2[M_2^2+2M_2M_1^2]\sum_{i,j}J_{ij}^2, \quad (72)$$

where we have used Eq. (45) to express $\langle\sigma^2\rangle$ in terms of the M_n's.

Equations (70) and (71) involve simple products of semi-invariants corresponding to the vertices in the associated diagrams. In Eq. (70) the diagrams involve two singly bonded vertices and the term involves M_1^2. Equation (71) is associated with three vertices; singly bonded, doubly bonded, and singly bonded. The corresponding term involves $M_1M_2M_1$.

Equation (72) has a more complex structure, involving $M_2^2+2M_2M_1$. It can be read from the diagram as follows: From the diagram (2,1) we first read M_2^2. If the diagram were opened on either the right or the left we would read $M_2M_1^2$. If the diagram were opened simultaneously on the left and right it would be unlinked, and we would write no contribution. Thus the proper combination of semi-invariants can be read from the diagram by successively considering it opened in every conceivable way which does not make it unlinked, and associating a simple product of semi-invariants with each such form of the diagram.

Now combining all two-bond diagrams, we obtain

$$-\beta F_2=-\beta F_{(2,1)}-\beta F_{(2,2)}=\tfrac{1}{4}(2\beta)^2M_2^2\sum_{i,j}J_{ij}^2$$
$$+\tfrac{1}{2}(2\beta)^2M_2M_1^2[\sum_{ij}J_{ij}^2+\sum_{ijk}{}'J_{ij}J_{jk}]$$
$$=\tfrac{1}{4}(2\beta)^2M_2^2\sum_{ij}J_{ij}^2+\tfrac{1}{2}(2\beta)^2M_2M_1^2\sum_{ijk}J_{ij}J_{jk}, \quad (74)$$

where the summations without primes permit unrestricted summation over indices.

The grouping of the restricted summations, coming from different classes of diagrams, to give an unrestricted summation in Eq. (74) is a general result. We shall demonstrate how this occurs for the three-bond diagrams.

The simple open-chain diagrams [(3,5) of Fig. 1] give

$$-\beta F_{(3,5)}=(2\beta)^3M_{(3,5)}\tfrac{1}{2}\sum_{i,j,k,l}{}'J_{ij}J_{jk}J_{kl}$$
$$=\tfrac{1}{2}(2\beta)^3M_1^2M_2^2\sum_{i,j,k,l}{}'J_{ij}J_{jk}J_{kl}. \quad (75)$$

The three-bond branched chain diagrams (3,4) give

$$-\beta F_{(3,4)}=(2\beta)^3M_{(3,4)}\tfrac{1}{6}\sum_{i,j,k,l}{}'J_{ij}J_{ik}J_{il}$$
$$=\tfrac{1}{6}(2\beta)^3M_3M_1^3\sum_{i,j,k,l}{}'J_{ij}J_{ik}J_{il}. \quad (76)$$

The triangular diagrams (3,3) give

$$-\beta F_{(3,3)}=(2\beta)^3M_{(3,3)}\tfrac{1}{6}\sum_{i,j,k}{}'J_{ij}J_{jk}J_{ki}$$
$$=\tfrac{1}{6}(2\beta)^3[\langle\sigma_1^2\sigma_2^2\sigma_3^2\rangle-3\langle\sigma_1\sigma_2\rangle\langle\sigma_1\sigma_2\sigma_3^2\rangle$$
$$+2\langle\sigma_1\sigma_2\rangle\langle\sigma_2\sigma_3\rangle\langle\sigma_3\sigma_1\rangle]\sum_{ijk}{}'J_{ij}J_{jk}J_{ki}$$
$$=\tfrac{1}{6}(2\beta)^3[M_2^3+3M_2^2M_1^2]\sum_{i,j,k}{}'J_{ij}J_{jk}J_{ki}. \quad (77)$$

Note that M_2^3 comes from the closed form of the diagram, whereas there are three ways of considering the diagram opened, each implying $M_2^2M_1^2$.

The diagrams of the type (3,2) give

$$-\beta F_{(3,2)}=(2\beta)^3M_{(3,2)}\tfrac{1}{2}\sum_{ijk}{}'J_{ij}^2J_{jk}$$
$$=\tfrac{1}{2}(2\beta)^3[M_2M_3M_1+M_1^2M_3M_1$$
$$+2M_2^2M_1^2]\sum_{ijk}{}'J_{ij}^2J_{jk}. \quad (78)$$

The first term in brackets corresponds to the closed form of the diagram, the second term corresponds to opening it on the left, and the third term corresponds to the fact that either the upper or the lower double bond can be opened at the center vertex.

Finally, the triple-bond diagrams (3,1) give

$$-\beta F_{(3,1)}=\frac{1}{3!2}(2\beta)^3[M_3^2+6M_3M_2M_1$$
$$+2M_3M_1^3+6M_2^2M_1^2]\sum_{ij}J_{ij}^3. \quad (79)$$

Adding all three-bond diagrams, we find

$$-\beta F_3=\tfrac{1}{12}(2\beta)^3[M_3^2\sum_{ij}J_{ij}^3+6M_3M_2M_1(\sum_{ijk}{}'J_{ij}^2J_{jk}+\sum_{ij}J_{ij}^2)+2M_2^3\sum_{ijk}{}'J_{ij}J_{jk}J_{ki}+2M_3M_1^3(\sum_{ijkl}{}'J_{ij}J_{ik}J_{il}+3\sum_{ijk}{}'J_{ij}^2J_{jk}+\sum_{ij}J_{ij}^3)+6M_2^2M_1^2(\sum_{ijkl}{}'J_{ij}J_{jk}J_{kl}+\sum_{ijk}{}'J_{ij}J_{jk}J_{ki}+2\sum_{ijk}{}'J_{ij}^2J_{jk}+\sum_{ij}J_{ij}^3)], \quad (80)$$

and we again note that the various summations within each set of parentheses combine to give unrestricted summations, so that

$$-\beta F_3=\tfrac{1}{12}(2\beta)^3M_3^2\sum_{ij}J_{ij}^3+\tfrac{1}{2}(2\beta)^3M_3M_2M_1\sum_{ijk}J_{ij}^2J_{jk}+\tfrac{1}{6}(2\beta)^3M_2^3\sum_{ijk}J_{ij}J_{jk}J_{ki}+\tfrac{1}{6}(2\beta)^3M_3M_1^3\sum_{ijkl}J_{ij}J_{ik}J_{il}+\tfrac{1}{2}(2\beta)^3M_2^2M_1^2\sum_{ijkl}J_{ij}J_{jk}J_{kl}. \quad (81)$$

Equations (70), (74) and (81) demonstrate our desired type of expansion, for the particular cases of one-bond, two-bond and three-bond clusters. The individual terms will be represented by diagrams, according to the following convention.

In Eq. (74), the term $\frac{1}{4}(2\beta)^2M_2^2\sum_{ij}J_{ij}^2$ will be represented henceforth by the diagram (2,1), and the term $\frac{1}{2}(2\beta)^2M_2M_1^2\sum_{ijk}J_{ij}J_{jk}$ will be represented henceforth by the diagram (3,5). Thus each diagram henceforth implies the factors $(2\beta)^nG_{n,t}{}^{-1}$, a simple product of semi-invariants corresponding to the individual vertices, and finally an unrestricted summation of a product of J_{ij}'s.

In Eq. (81), the five terms are successively represented by the diagrams (3,1), (3,2), (3,3), (3,4), (3,5), and it can be corroborated easily that the terms are associated with these new types of diagrams by the convention explained above.

We now discuss the general features of this regrouping of terms, so that each new type of term (represented by a new type of diagram) involves a simple product of semi-invariants and an unrestricted summation of J_{ij}'s.

5. THE REARRANGED EXPANSION

The specific examples above have demonstrated the general features of a rearrangement of the terms of Eq. (69), leading to a new type of expansion. This rearrangement does not mix terms of different n (where n is number of bonds); we therefore fix our attention on the various terms of a given n in Eq. (69). Each term corresponds to a particular topological type of diagram and consists of three factors: a weight factor $(2\beta)^nG_{n,t}{}^{-1}$, a quantity $M_{(n,t)}$, and a restricted sum of products of exchange integrals. The restriction in this latter sum prevents the various indices from taking common values. After the rearrangement, the terms again correspond to particular topological types of diagrams and consist of three factors: the same weight factor $(2\beta)^nG_{n,t}{}^{-1}$, and a product of semi-invariants of single spins (with degrees corresponding to the number of bonds joined to that spin in the diagram), and an unrestricted sum of products of exchange integrals.

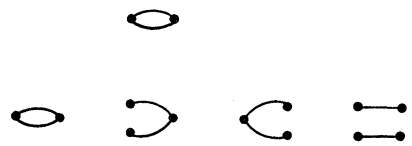

FIG. 2. Opening of the old-type diagram at top [by Eq. (82)] gives the four new-type diagrams shown.

The essential step in the rearrangement of terms is the decomposition of the quantity $M_{(n,t)}$ into a sum of products of semi-invariants of single spins, these individual products then being reclassified among the diagrams of various topological type.

Consider a representative quantity $M_{(n,t)}$; it is the sum of products of averages of spin deviation operators. The leading term is a simple average of all the σ_j's represented in the diagram, and the remaining terms subtract all possible opened forms (i.e., separately averaged factors) so as to insure the vanishing of unlinked diagrams.

Each term in $M_{(n,t)}$ can be written as a sum of products of single-spin semi-invariants, and each of these terms corresponds to one of the new-type diagrams. Thus, $\langle\sigma_1^2\sigma_2^2\rangle$ [which is the leading term in the old-type diagram (2,1)] can be written as

$$[M_2(1)+M_1^2(1)][M_2(2)+M_1^2(2)]=M_2(1)M_2(2)+M_1^2(1)M_2(2)+M_2(1)M_1^2(2)+M_1^2(1)M_1^2(2)$$

associated with the four new-type diagrams[13] shown in Fig. 2. In general, this decomposition into terms associated with new-type diagrams can be accomplished by using Eq. (44) to write

$$\langle\sigma_k{}^n\rangle=[D_k+M_1(k)]^{n-1}M_1(k). \quad (82)$$

This equation is subject to a direct interpretation, for we note that

$$[D_k+M_1(k)]M_m(k)=M_{m+1}(k)+M_1(k)M_m(k).$$

Thus if a site has m bonds attached to it, and if we operate with $D_k+M_1(k)$, we generate a site with $m+1$ bonds and an opened site. Consequently, at each step in the building up of the term $\langle\sigma_k{}^n\rangle$ in Eq. (82) we introduce the possibility of the new bond being either closed or opened at the site k. In this way the leading term in an old-type diagram generates a series of new-type terms corresponding to every possible way of

[13] It should also be noted that the remaining term corresponding to the old-type diagram (2,1) is $-\langle\sigma_1\sigma_2\rangle^2=-M_1^2(1)M_1^2(2)$, which subtracts away the unlinked new-type diagram of Fig. 2.

opening each vertex in the original diagram. The remaining terms in $M_{(n,t)}$ then subtract away all unlinked diagrams. Hence we arrive at the result which we have demonstrated in particular cases above:

The spin factor $M_{(n,t)}$ of an old-type diagram can be written as a sum of spin factors $M_p(1)M_m(2)\cdots$ corresponding to new-type diagrams. The new-type spin factors correspond to each way of opening the original diagram, ignoring all unlinked diagrams.

Symbolically, we write

$$M_{(n,t)}=\sum_{t'} A_{tt'}\tilde{M}_{(n,t')}, \tag{83}$$

where $\tilde{M}_{(n,t')}$ is a product of semi-invariants of single spins such that every p-bonded vertex in the diagram is represented by a factor $M_p(\sigma)$, and $A_{tt'}$ is the number of ways of opening the diagram (n,t) to obtain the diagram (n,t').

The second aspect of the rearrangement of the cluster expansion involves collecting all terms with similar spin averages of the new type. We therefore substitute Eq. (83) into the cluster expansion, Eq. (69).

$$-\beta F'=\sum_{ntt'}(2\beta)^n G_{n,t}^{-1}A_{tt'}\tilde{M}_{(n,t')}\sum_{(t)}{}' J_{ij}J_{kl}\cdots, \tag{84}$$

where the final summation is over the summation indices, which reflect the pattern of the diagram t.

Collecting terms with similar $\tilde{M}_{(n,t')}$, we have

$$-\beta F'=\sum_{n,t'}(2\beta)^n G_{n,t'}{}^{-1}\tilde{M}_{(n,t')}\mathcal{J}_{n,t'}, \tag{85}$$

where

$$\mathcal{J}_{n,t'}=\sum_{t}\frac{G_{n,t'}}{G_{n,t}}A_{t,t'}\sum_{(t)}{}' J_{ij}J_{kl}\cdots. \tag{86}$$

The summation in Eq. (86) is over all classes of diagrams t which can be *opened* to produce t'. It includes the particular term $t=t'$, and all other diagrams t which are more closed than t'. We indicate this explicitly by splitting off the term $t=t'$, to write

$$\mathcal{J}_{n,t'}=\sum_{(t')}{}' J_{ij}J_{kl}\cdots+\sum_{t<t'}\frac{G_{n,t'}}{G_{n,t}}A_{t,t'}\sum_{(t)}{}' J_{ij}J_{kl}\cdots. \tag{87}$$

We now wish to show that the second term in this equation can be absorbed into the first term merely by removing the restriction on the first summation. That is, $\mathcal{J}_{n,t'}$ is the unrestricted sum of a product of J_{ij}'s, with a pattern of indices corresponding to the diagram (n,t'):

$$\mathcal{J}_{n,t'}=\sum_{i,j,k,l\cdots}J_{ij}J_{kl}\cdots. \tag{88}$$

In order to establish this result, we consider the effect of removing the restrictions on the summation in the first term of Eq. (87). Some sets of indices thereby become equal, corresponding to diagrams t of greater closure. The number of such diagrams is clearly equal to the number of ways of closing the diagram t' to obtain t. Let this number of ways of closing t' to t be denoted by $A_{t',t}$. Then it would follow that these additional terms, introduced by removal of the restrictions on the summation, are precisely supplied by the second term in Eq. (87), if we could show that

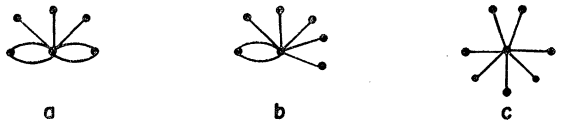

FIG. 3. A more-closed diagram (a) and two types of more-open diagrams (b) and (c) obtained from it.

$$A_{t',t}=(G_{n,t'}/G_{n,t})A_{t,t'}. \tag{89}$$

To prove this relation we proceed to count the number of ways of opening the diagram (n,t) to produce the diagram (n,t'); that is, we compute $A_{t,t'}$. For simplicity we consider first the case in which the diagram (n,t) must be opened at only a single point, as, for instance, Fig. 3(a) being opened to Fig. 3(b) (with $A_{t,t'}=2$ and $A_{t',t}=10$ in this case). Now let us suppose that we agree to open the diagram at a particular location, obtaining the various ways of opening the diagram by rotating or reflecting or permuting the diagram so as to bring various equivalent elements to the appointed location. We can count the number of ways of opening the diagram by counting the number of permutation operations which bring new (but equivalent) elements to this location. This number of permutations clearly is equal to the total number of permutations of the diagram $G_{n,t}$ divided by the number of permutations which do *not* bring new elements to the location, G'. This latter number G' can be thought of as the order of the symmetry group of the diagram if one of the elements to be opened is held fixed at the appointed location. Thus we have found that $A_{tt'}=G_{n,t}/G'$. We now compute the number of ways of closing the diagram (n,t') to produce (n,t), using the same device. Again we bring certain elements to the appointed location, where they will be joined together. The number of ways of doing this is equal to the total number of permutations $G_{n,t'}$, divided by the number of permutations if a given set of elements is held fixed at the location; again G'. Hence $A_{t't}=G'_{n,t}/G'$, and from these relations we immediately corroborate Eq. (89).

If there is more than one location at which the diagram (n,t) must be opened, as in opening Fig. 3(a) to produce Fig. 3(c), then the above formulas for both $A_{tt'}$ and $A_{t't}$ must be divided by G''. Here G'' is the number of permutations among equivalent cutting locations. The relationship (89) clearly remains valid.

To summarize, then, we have established the following expansion for $-\beta F'$

$$-\beta F'=\sum_{n,t}(2\beta)^n G_{n,t}{}^{-1}\tilde{M}_{(n,t)}\mathcal{J}_{n,t}. \tag{90}$$

Here (n,t) designates a topological type of diagram consisting of n bonds and the sum is over all topologically distinct diagrams. $G_{n,t}$ is the order of the symmetry group of the diagram (n,t). $\bar{M}_{(n,t)}$ is a product of semi-invariants of single spins such that each p-bonded vertex in the diagram is represented by a factor M_p. $\mathcal{J}_{n,t}$ is the unrestricted sum of a product of J_{ij}'s, the pattern of summation indices on the J_{ij}'s corresponding to the pattern of bonds in the diagram. A diagram henceforth denotes the corresponding term in Eq. (90).

6. CLASSIFICATION OF DIAGRAMS

As in all diagrammatic methods, only limited subsets of diagrams can be summed. The essence of the approximation scheme lies in the criterion for the selection of the dominant sets of diagrams. At this point we are not yet in a position fully to develop such a criterion, but it is desirable to indicate in a rough way the types of diagrams which are apt to be most important, so as to focus and guide the development of the theory.

In succeeding sections we shall find it essential to renormalize the vertices in the diagrams, so that each vertex will represent not a single spin, but entire complexes of linked spins. Each renormalized diagram will then represent a large number (in fact, an infinite number) of unrenormalized diagrams. The criterion for the selection of subsets of diagrams will be formulated in terms of these renormalized diagrams, and we shall find that the nth order correction to the free energy arises from the summation of renormalized diagrams containing n loops. In order to motivate this classification we review an argument due to Brout.[11] In its original form this argument ostensibly applies to the unrenormalized diagrams, and we so present it here. In the following sections we shall find that it fails for the unrenormalized diagrams, but it nevertheless guides the development of the renormalization procedure.

Brout bases his classification on two observations. First, if the range of interaction is infinite (so that each spin interacts equally strongly with every other spin in the lattice) the rigorous solution of the Ising problem is the Bragg-Williams or molecular field solution, and it is observed that in the actual physical case the molecular field solution is at least qualitatively successful. The second observation is that even with short-range interactions each spin in a three-dimensional lattice interacts with a rather large number of other spins (eight for a bcc structure, and twelve for an fcc structure). Brout has therefore suggested an expansion in powers of $1/z$, where z is the effective number of spins with which a given spin interacts.

A convenient definition of z is obtained by equating J_0 to Jz, where J is the value of J_{ij} when i and j are nearest neighbors:

$$J_0 \equiv Jz. \tag{91}$$

Equivalently,

$$z = z_1 + r_2 z_2 + r_3 z_3 + \cdots, \tag{92}$$

where z_1 is the number of nearest neighbors, z_2 is the number of second-nearest neighbors, etc., and where r_2 is the ratio of the exchange integral J_{ij} for second-nearest neighbors to its value J for nearest neighbors.

The Curie temperature is at least roughly determined by equating kT_c to the energy required to invert one spin:

$$2J_0 S^2 \simeq kT_c, \tag{93}$$

or

$$(2\beta_c J)S^2 \simeq 1/z. \tag{94}$$

If we now recall the contribution of each bond to a diagram, we note that each bond contributes a factor $2\beta J_{ij}$, as well as influencing the spin-dependent factors (semi-invariants) at its termini. We temporarily associate these contributions to the semi-invariants with the factor S^2 in Eq. (94), thereby identifying the contribution of each bond to a diagram as having a value of the order of $1/z$. However, one of the summation indices in $\mathcal{J}_{n,t}$ can take N values, and each other index summed in $\mathcal{J}_{n,t}$ can take z values effectively. Hence, a completely open diagram, with n bonds and $(n+1)$ free summation indices, is classified as zero order in $1/z$. A diagram containing one closed loop, with n bonds and n free summation indices, is classified as first order in $1/z$. Diagrams containing two closed loops, such as (3,1) or (4,3) of Fig. 1, are classified as of order $(1/z)^2$.

Two points in the above argument are obviously inadequate. Equation (93) for the Curie temperature is not accurate, and the contribution of each bond to the semi-invariants at its termini is certainly not adequately represented by the factors S^2. Correction of these factors will be made in terms of the renormalization techniques, and we shall find that Brout's $1/z$ criterion is more reliably stated in terms of the renormalized diagrams. At this point we use the above considerations to indicate that the most open diagrams are apt to be the most significant physically.

7. ZERO-ORDER DIAGRAMS: THE MOLECULAR FIELD

We shall now show that summation of all diagrams of zero order, or Cayley trees, leads to the familiar molecular field approximation. Direct summation of these diagrams is carried out in Appendix A, but we here utilize an alternative and much simpler procedure. We show that it is possible to choose the hitherto undetermined parameter $\bar{S}$ in such a way that all Cayley trees vanish identically. This choice of $\bar{S}$ transfers all contributions of zero order into the unperturbed contribution $-\beta F_0$, which we have already computed.

Every Cayley tree, having a free end, contains a factor $M_1(\sigma)$. Choosing $\bar{S}$ so that $M_1=0$ therefore eliminates all such diagrams. Accordingly, we determine

$\bar{S}$ by

$$M_1(\sigma)=\langle\sigma\rangle=\langle\bar{S}-S_z\rangle=\bar{S}-\langle S_z\rangle=\bar{S}-M_1(S_z)=0, \quad (95)$$

or denoting this value of $\bar{S}$ by $\bar{S}_0$,

$$\bar{S}_0=\langle S_z\rangle=\sum_{-S}^{S} S_z \exp(\beta LSS_z)/\sum_{-S}^{S}\exp(\beta LSS_z) =SB_s(\beta LS), \quad (96)$$

where $B_s(x)$ is the Brillouin function for spin S,

$$B_s(x)=\frac{1}{2S}\left\{(2S+1)\coth\left[\left(\frac{2S+1}{2S}\right)x\right] -\coth\left(\frac{x}{2S}\right)\right\}. \quad (97)$$

It is to be observed that quantities are conveniently expressed sometimes in terms of spin variables σ_i and sometimes in terms of S_{iz}. Semi-invariants can be written in terms of either variable, $M_n(\sigma)$ or $M_n(S_z)$. From the properties of semi-invariants given in Eqs. (37)–(39), we have $M_n(\sigma)=M_n(S_z)$ for n even and $M_n(\sigma)=-M_n(S_z)$ for $n>1$ and odd; for $n=1$, $M_1(\sigma)=\bar{S}-M_1(S_z)$. In the following, either $M_n(\sigma)$ or $M_n(S_z)$ may be indicated simply by M_n in those places in which its specific meaning is clear by context.

From Eq. (16) we now have

$$-\beta F_0=-N\beta J_0\bar{S}_0^2+N\ln\sinh[\beta L(S+\tfrac{1}{2})] -N\ln\sinh(\tfrac{1}{2}\beta L), \quad (98)$$

and the magnetization is, to this approximation,

$$\mathfrak{M}_0=-\partial F_0/\partial H=g\mu_0 N\langle S_z\rangle=g\mu_0 N\bar{S}_0 =g\mu_0 NSB_s(\beta LS). \quad (99)$$

This, of course, is the familiar result of the Weiss internal field approximation, and from Eq. (7) we identify the Weiss field as $2J_0\bar{S}/g\mu_0$.

It is useful to write the expressions for the magnetic susceptibility and the specific heat for comparison with later results. The susceptibility is, to zero order,

$$\chi_0=(1/N)(\partial\mathfrak{M}_0/\partial H)=g\mu_0(\partial\bar{S}_0/\partial H), \quad (100)$$

where

$$\frac{\partial\bar{S}_0}{\partial H}=\frac{\partial M_1(S_z)}{\partial H}+\frac{\partial M_1(S_z)}{\partial\bar{S}_0}\frac{\partial\bar{S}_0}{\partial H}, \quad (101)$$

and where $\partial M_1/\partial H$ implies constant $\bar{S}_0$, and $\partial M_1/\partial\bar{S}_0$ implies constant H. Thus

$$\frac{\partial\bar{S}_0}{\partial H}=\frac{g\mu_0\beta M_2}{1-2\beta J_0 M_2}. \quad (102)$$

Inserting Eq. (102) into (100) we obtain

$$\chi_0=(g\mu_0)^2\beta M_2/(1-2\beta J_0 M_2). \quad (103)$$

The specific heat is obtained from

$$c_{V0}=\frac{\partial E_0}{\partial T}=-k\beta^2\frac{\partial E_0}{\partial\beta}=Nk\beta^2[2J_0\bar{S}_0+g\mu_0 H]\frac{\partial\bar{S}_0}{\partial\beta}, \quad (104)$$

where

$$\frac{\partial\bar{S}_0}{\partial\beta}=\frac{\partial M_1(S_z)}{\partial\beta}+\frac{\partial M_1(S_z)}{\partial\bar{S}_0}\frac{\partial\bar{S}_0}{\partial\beta}, \quad (105)$$

with $\bar{S}_0$ constant in the differentiation of M_1 with respect to β, and β constant in the differentiation with respect to $\bar{S}_0$. Thus

$$\partial\bar{S}_0/\partial\beta=(2J_0\bar{S}_0+g\mu_0 H)M_2/(1-2\beta J_0 M_2). \quad (106)$$

Thus the specific heat becomes

$$c_{V0}=Nk[2\beta J_0\bar{S}_0+g\mu_0\beta H]^2 M_2/(1-2\beta J_0 M_2). \quad (107)$$

There remains one important formal property of the expression for F_0, which should be noted. Before committing ourselves to a choice of $\bar{S}$ we might have inquired as to the dependence of F_0 on this undetermined parameter. Then from Eq. (15)

$$\partial F_0/\partial\bar{S}=2NJ_0[\bar{S}-\langle S_z\rangle], \quad (108)$$

and the choice of $\bar{S}$ for which

$$\partial F_0/\partial\bar{S}=0 \quad (109)$$

is $\bar{S}=\bar{S}_0=\langle S_z\rangle$.

Consequently the choice of $\bar{S}$ which we made for analytic convenience, in Eq. (95), is the "best" choice of $\bar{S}$. To summarize, then, we have found that the choice of $\bar{S}$ which eliminates diagrams of the zero order has two important physical properties. It is equal to the average value of S_z, evaluated to zero order. And it minimizes the free energy to that order. These properties will be important guides to the choice of $\bar{S}$ in higher order.

8. SUMMATION OF FIRST-ORDER DIAGRAMS

The straightforward procedure for improving the zero-order approximation is the summation of all diagrams in Eq. (90) which, according to Brout's criterion, would be of first order in $1/z$. This is very easily done, but as we shall see, it leads to an unsatisfactory result. The procedure is of interest, nevertheless, because analysis of the cause of its failure suggests the renormalization procedure which provides a satisfactory solution of the problem.

We consider those diagrams in Eq. (90) with a single closed loop. To this loop there can be appended an arbitrary number of branched or unbranched chains; however, the choice of $\bar{S}$ which we have adopted eliminates all such chains and leaves only the bare loops. For $n=2, 3, 4, \cdots$ these single-loop diagrams are, respectively, a double bond, a triangle, a square, etc.

The symmetry of an n-sided polygon consists of an n-fold rotation and a reflection, so that the order of the

group is $G_{n,t}=2n$. Alternatively, there are $2n$ ways of numbering the vertices, as we can assign the number 1 to any of the n vertices, and then proceed with the numbers 2, 3, $4\cdots$ in either clockwise or counterclockwise order. Thus,

$$-\beta F^{(1)}=\sum_{n=2}^{\infty}(2\beta)^n\frac{1}{2n}M_2{}^n\sum_{i,j,k\cdots}J_{ij}J_{jk}\cdots J_{li}. \quad (110)$$

Let

$$\begin{aligned}\mathbf{r}_j-\mathbf{r}_i&=\boldsymbol{\delta}_1,\\ \mathbf{r}_k-\mathbf{r}_j&=\boldsymbol{\delta}_2,\\ &\vdots\\ \mathbf{r}_i-\mathbf{r}_l&=\boldsymbol{\delta}_n,\end{aligned} \quad (111)$$

where $\mathbf{r}_i$ is the vector position of the ith site. Then, assuming that the exchange integrals $J_{ij}=J_{\delta_1}$ depends only on the vector distance $\boldsymbol{\delta}_1$ between the sites (and not on $\mathbf{r}_i$ as well), the summation over the indices $i, j, k\cdots$ can be replaced by

$$\sum_{i,j,k\cdots}J_{ij}J_{jk}\cdots J_{li}=N\sum_{\delta_1,\delta_2\cdots\delta_n}J_{\delta_1}J_{\delta_2}\cdots J_{\delta_n}, \quad (112)$$

with the restriction that

$$\boldsymbol{\delta}\equiv\boldsymbol{\delta}_1+\boldsymbol{\delta}_2+\cdots+\boldsymbol{\delta}_n=0. \quad (113)$$

This restriction on the sum of the $\boldsymbol{\delta}$'s insures the closure of the chain, to make a loop. This condition can be incorporated into Eq. (112) by introducing the representation of the Kronecker delta,

$$\frac{1}{N}\sum_{\mathbf{q}}\exp(i\mathbf{q}\cdot\boldsymbol{\delta})=\begin{cases}1 & \text{if } \boldsymbol{\delta}=0\\ 0 & \text{if } \boldsymbol{\delta}\neq 0,\end{cases} \quad (114)$$

where the $\mathbf{q}$ ranges over the Brillouin zone, taking the discrete values of the reduced, rationalized, reciprocal lattice. Then

$$\sum_{ijk\cdots}J_{ij}J_{jk}\cdots J_{li}=\sum_{\mathbf{q}}\sum_{\delta_1,\delta_2\cdots}J_{\delta_1}J_{\delta_2}\cdots \times J_{\delta_n}\exp[i\mathbf{q}\cdot(\boldsymbol{\delta}_1+\boldsymbol{\delta}_2+\cdots+\boldsymbol{\delta}_n)] \quad (115)$$

$$=\sum_{\mathbf{q}}J^n(\mathbf{q}), \quad (116)$$

where $J(\mathbf{q})$ is the $\mathbf{q}$th Fourier component of J_δ,

$$J(\mathbf{q})=\textstyle\sum_\delta J_\delta\exp(i\mathbf{q}\cdot\boldsymbol{\delta}), \quad (117)$$

and where, in carrying out this summation, it is to be recalled that for $\boldsymbol{\delta}=0$, J_δ has been defined as zero. This has the consequence that

$$\textstyle\sum_{\mathbf{q}}J(\mathbf{q})=J_{\delta=0}=0. \quad (118)$$

Equations (116) and (118), which will prove to be very convenient, have a simple interpretation.[11] The quantities J_{ij} can be considered as elements of an $N\times N$ matrix. The elements of this matrix are translationally invariant, from which it follows that the eigenvectors transform according to the irreducible representations of the translation group of the lattice. The ith element of the $\mathbf{q}$th eigenvector therefore is $e^{i\mathbf{q}\cdot\mathbf{r}_i}$, and the $\mathbf{q}$th eigenvalue is $J(\mathbf{q})$. Equation (116) represents the trace of the nth power of the matrix, which is equal to the sum of the nth powers of its eigenvalues. The diagonal values of the matrix, J_{ii}, vanish, so that the trace of the matrix, and hence the sum of its eigenvalues, vanishes, as in Eq. (118).

Inserting Eq. (116) into Eq. (110) we now find the contribution of the first-order diagrams to be

$$-\beta F^{(1)}=\sum_{\mathbf{q}}\sum_{n=1}^{\infty}\frac{1}{2n}[2\beta M_2J(\mathbf{q})]^n, \quad (119)$$

where the inclusion of the term for $n=1$ is justified by Eq. (118). Carrying out the summation

$$-\beta F^{(1)}=-\tfrac{1}{2}\textstyle\sum_{\mathbf{q}}\ln[1-2\beta J(\mathbf{q})M_2]. \quad (120)$$

Combining this first-order contribution with the zero-order contribution [Eq. (15)], the free energy to first order is

$$-\beta F_1=-\beta(F_0+F^{(1)})=-\beta NJ_0\bar{S}_0{}^2+N\ln\sum_{-S}^{S}e^{\beta LS_z}-\tfrac{1}{2}\sum_{\mathbf{q}}\ln[1-2\beta J(\mathbf{q})M_2]. \quad (121)$$

The magnetization is, to first order,

$$\mathfrak{M}_1=-\frac{\partial F_1}{\partial H}=Ng\mu_0\left[\bar{S}_0+\frac{1}{g\mu_0\beta}\Gamma\frac{\partial M_2}{\partial H}\right], \quad (122)$$

where

$$\Gamma=\frac{1}{2N}\sum_{\mathbf{q}}\frac{2\beta J(\mathbf{q})}{1-2\beta J(\mathbf{q})M_2}. \quad (123)$$

But for any n

$$\partial M_n/\partial H=(\partial M_n/\partial H)+(\partial M_n/\partial\bar{S})_H\partial\bar{S}/\partial H, \quad (124)$$

the first derivative on the right being taken at constant $\bar{S}$. Furthermore, noting that the density function with respect to which the spin averages are taken in $M_n(S_z)$ is of the form $e^{\beta LS_z}=\exp[\beta(g\mu_0H+2J_0\bar{S})S_z]$, and comparing this form with the ρ_α defined in Eq. (23), we can introduce a D operator by the definitions

$$D=(1/\beta g\mu_0)(\partial/\partial H), \quad (\bar{S}\text{ constant}), \quad (125)$$

and

$$D=(1/2\beta J_0)(\partial/\partial\bar{S})_H. \quad (126)$$

This new D operator is the negative of the D_α operator previously defined and used; accordingly, it generates the $M_n(S_z)$ rather than the $M_n(\sigma)$, by the equation $M_{n+1}(S_z)=DM_n(S_z)$. In this connection the comments just below Eq. (97) should be recalled. Henceforth we shall use the notation D for either type of operator, implying always that D appropriate to the type of spin

operator in the context. Hence, by Eqs. (31) and (102),

$$\frac{\partial M_n(S_z)}{\partial H}=g\mu_0\beta M_{n+1}+2\beta J_0 M_{n+1}\frac{g\mu_0\beta M_2}{1-2\beta J_0 M_2} \quad (127)$$

$$=g\mu_0\beta\frac{M_{n+1}(S_z)}{1-2\beta J_0 M_2(S_z)}, \quad (128)$$

and inserting this into Eq. (122),

$$\mathfrak{M}_1=g\mu_0 N\left[\bar{S}_0+\frac{M_3\Gamma}{1-2\beta J_0 M_2}\right]$$

$$=g\mu_0 N\left[M_1+\frac{M_3\Gamma}{1-2\beta J_0 M_2}\right]. \quad (129)$$

The susceptibility is

$$\chi_1=\frac{1}{N}\frac{\partial\mathfrak{M}_1}{\partial H}=g\mu_0^2\beta\left[\frac{M_2}{1-2\beta J_0 M_2}\right.$$

$$\left.+\frac{M_4\Gamma+M_3^2\Delta}{(1-2\beta J_0 M_2)^2}+\frac{2\beta J_0 M_3^2\Gamma}{(1-2\beta J_0 M_2)^3}\right], \quad (130)$$

where

$$\Delta=\frac{1}{2N}\sum_{\mathbf{q}}\left(\frac{2\beta J(\mathbf{q})}{1-2\beta J(\mathbf{q})M_2}\right)^2, \quad (131)$$

and where Eq. (128) has again been used to carry out the indicated differentiation.

From Eq. (130) we find that the susceptibility diverges at $2\beta_c J_0 M_2=1$, or at the same temperature as in zero order. However, this is not a satisfactory solution, as we shall now find by an examination of the behavior of the magnetization at this temperature.

The second term in the magnetization is $M_3\Gamma/(1-2\beta J_0 M_2)$. The factor Γ is well-behaved as the temperature approaches the Curie temperature; the denominator vanishes as $\beta\rightarrow\beta_c$, and the factor M_3 also vanishes. This latter fact follows from the definition of M_3 in terms of averages of odd powers of S_z, which vanish at (and above) the Curie temperature. Consequently, we must carefully consider the ratio $M_3/(1-2\beta_c J_0 M_2)$. To do so we assume a small magnetic field to be present and we expand in powers of this field:

$$\lim_{H\rightarrow 0}\frac{M_3+(\partial M_3/\partial H)H}{1-2\beta_c J_0[M_2+(\partial M_2/\partial H)H]}=\frac{\partial M_3/\partial H}{-2\beta_c J_0(\partial M_2/\partial H)}$$

$$=\frac{g\mu_0 M_4}{1-2\beta_c J_0 M_2}\left(-2\beta_c J_0\frac{g\mu_0 M_3}{1-2\beta_c J_0 M_2}\right)^{-1}$$

$$=\frac{M_4}{-2\beta_c J_0 M_3}, \quad (132)$$

where we have again used Eq. (128) in order to carry out the differentiations. But M_4 involves averages of even powers of S_z and does not vanish at $\beta=\beta_c$, whereas M_3 does vanish. Hence the magnetization is divergent at the Curie temperature.

The divergence of the magnetization can be shown explicitly for the case of spin $\frac{1}{2}$. The semi-invariants in this case are

$$M_1=\langle S_z\rangle=\tfrac{1}{2}\tanh(\tfrac{1}{2}\beta L), \quad (133)$$

$$M_2=\tfrac{1}{4}\operatorname{sech}^2(\tfrac{1}{2}\beta L), \quad (134)$$

$$M_3=-2M_1M_2. \quad (135)$$

The Curie temperature is defined by

$$2\beta_c J_0 M_2=\tfrac{1}{2}\beta_c J_0[\operatorname{sech}^2(\tfrac{1}{2}\beta L)]_{L\rightarrow 0}=1, \quad (136)$$

or

$$\beta_c J_0=2. \quad (137)$$

The quantity of interest in the magnetization is

$$\frac{M_3}{1-2\beta_c J_0 M_2}=\lim_{L\rightarrow 0}\frac{-\tfrac{1}{4}\tanh(\tfrac{1}{2}\beta L)\operatorname{sech}^2(\tfrac{1}{2}\beta L)}{1-2\beta_c J_0[\tfrac{1}{4}\operatorname{sech}^2(\tfrac{1}{2}\beta L)]} \quad (138)$$

$$=-\tfrac{1}{4}\lim_{L\rightarrow 0}\frac{\tanh(\tfrac{1}{2}\beta L)\operatorname{sech}^2(\tfrac{1}{2}\beta L)}{1-\operatorname{sech}^2(\tfrac{1}{2}\beta L)} \quad (139)$$

$$=-\tfrac{1}{4}\lim_{L\rightarrow 0}[\sinh(\tfrac{1}{2}\beta L)\cosh(\tfrac{1}{2}\beta L)]^{-1}$$

$$=\infty. \quad (140)$$

One might, perhaps, surmise that the divergence of the magnetization arises from some subtlety in the manner in which we have approached the limit $N\rightarrow\infty$. Specifically, the upper limit $n=\infty$ in Eq. (119) implies that closed loops of unbounded length can be drawn in a lattice, whereas the true upper limit is of the order of N. However, let us not specify this upper limit, and merely substitute the sum (119) for the last term in Eq. (121). Then the magnetization becomes

$$\mathfrak{M}_1=Ng\mu_0\bar{S}_0-\tfrac{1}{2}\beta^{-1}\sum_{\mathbf{q}}\sum_n\frac{1}{2n}\frac{\partial}{\partial H}[2\beta J(\mathbf{q})M_2]^n \quad (141)$$

$$=Ng\mu_0\bar{S}_0-\tfrac{1}{4}\beta^{-1}M_2^{-1}\frac{\partial M_2}{\partial H}\sum_{\mathbf{q}}\sum_n[2\beta J(\mathbf{q})M_2]^n, \quad (142)$$

and the quantity $\partial M_2/\partial H$ is precisely the quantity which, as we have seen, diverges. Hence the divergence is quite independent of the process of taking $N\rightarrow\infty$.

Finally, we note two aspects of the solution to first order. Whereas in zero order $\bar{S}$ represented the magnetization, we see from Eq. (129) that it does not do so to first order. Secondly, whereas F_0 was minimum with respect to variations in $\bar{S}$, F_1 is not. For

$$\frac{\partial F_1}{\partial\bar{S}}=2NJ_0[\bar{S}-M_1(S_z)]$$

$$-\tfrac{1}{2}\beta^{-1}\sum_{\mathbf{q}}\frac{\partial}{\partial\bar{S}}\ln[1-2\beta J(\mathbf{q})M_2] \quad (143)$$

$$=2NJ_0\Big[\bar{S}-M_1(S_z)-\frac{1}{2N}\sum_{\mathbf{q}}\frac{2\beta J(\mathbf{q})}{1-2\beta J(\mathbf{q})M_2}M_3\Big] \quad (144)$$

$$=2NJ_0[\bar{S}-M_1(S_z)-M_3(S_z)\Gamma]\neq 0, \quad (145)$$

where we have used the relation (126) to carry out the differentiation. Now F is clearly independent of $\bar{S}$, and we should expect that $\partial F_n/\partial\bar{S}$ should vanish to every order in a consistent expansion. The fact that F_1 is not minimum with respect to $\bar{S}$ is an indication of an improper classification of diagrams, and it provides us with a guide to the reclassification which eliminates the divergence in the magnetization.

9. RENORMALIZATION; ELIMINATION OF $\bar{S}$-REDUCIBLE DIAGRAMS

Preparatory to generalizing the method of elimination of diagrams by appropriate choice of $\bar{S}$, it is convenient to review the standardized diagram terminology as used, for instance, by Uhlenbeck and co-workers.[14]

A vertex of a diagram is called an *articulation point* if the diagram can be severed into disjoint parts by a single cut at that vertex. A linked diagram having one or more articulation points is called a *tree*, whereas a linked diagram having no articulation points is called a *star*. Thus every tree can be thought of as composed of stars joined together at articulation points.

Trees can be classified according to the types of stars of which they are built. A *Cayley tree* is a tree for which every star is a simple bond, and consequently every vertex is an articulation point (or a terminal vertex); these are the diagrams which were summed in Appendix A. A *Husimi tree* is a tree composed of stars which are simply polygons or "loops." Another tree of particular interest to us is that for which every star is either a simple bond or a loop, such as (4,6) of Fig. 1; we shall refer to these as *Cayley-Husimi* trees.

Returning now to the analysis proper, we can describe our procedure as follows. The summation of Cayley trees, as carried out in Appendix A, is equivalent to the method of Sec. 7, in which all Cayley trees were eliminated by the choice of $\bar{S}$. The diagrams classified provisionally as first order in $1/z$ were the Cayley-Husimi trees consisting of a single loop and appended chains of bonds, but the choice of $\bar{S}$ reduced these only to simple loop stars, which were then summed in Sec. 8. Because this procedure did not prove to be satisfactory, we now consider the possibility of eliminating a much wider class of diagrams by a different choice of the parameter $\bar{S}$.

The diagrams which we shall eliminate by the new choice of $\bar{S}$ consist of all diagrams having a single bond joined to an articulation point; we call such diagrams *$\bar{S}$-reducible*. The $\bar{S}$-reducible diagrams can be considered to be composed of $\bar{S}$-irreducible diagrams connected together by single-bond chains. It is useful to refer to these $\bar{S}$-irreducible substructures as *hypervertices* of various types. The single bonds joining these hypervertices in an $\bar{S}$-reducible diagram can also be considered to be of various types, corresponding to the types of hypervertices at their ends. To stress this classification of the bonds we refer to them as *hyperbonds*. If we then think of the $\bar{S}$-reducible diagrams as chains of hyperbonds and hypervertices, they form an evident generalization of the Cayley trees.

Consider the class of $\bar{S}$-reducible diagrams composed of a prescribed class of hypervertices and connecting hyperbonds. These diagrams can be generated and summed by the following method. A given type of hypervertex is selected as a generator, and this generator is considered as unique and distinguishable from all other hypervertices which may subsequently be joined to it; such a distinguishable structural element is called a *root*. The general set of $\bar{S}$-reducible diagrams is built up by adding hypervertices and hyperbonds to this root, just as the Cayley trees were built in Appendix A. We shall later describe this synthesis process in greater detail, but we now assume that the total free-energy contribution from the complete set of rooted diagrams is computed. This is not the true free energy from the desired class of $\bar{S}$-reducible diagrams, because the selection of a unique root introduces certain errors. However, as shown in Appendix B, these errors are eliminated by repeating the calculation using every separate type of hypervertex as root and every separate type of hyperbond as root; subtraction of the contributions generated from all hyperbonds from the contributions generated from all hypervertices gives the proper free-energy contribution.

Consider the synthesis of rooted diagrams generated from a specific type of hypervertex as root. Let $-\beta F_\alpha$ be the contribution of this (type α) hypervertex itself, considered as a diagram. To generate $\bar{S}$-reducible diagrams from this hypervertex we first add one or more single bonds to each of the vertices of the hypervertex; this is accomplished by replacing every $M_n(\sigma)$ in $-\beta F_\alpha$ by $\exp[2\beta J_0 M_1(\sigma)D]M_n(\sigma)$, where we interpret $\exp[2\beta J_0 M_1(\sigma)D]$ as $\sum(n!)^{-1}(2\beta J_0 M_1(\sigma))^n D^n$. The linear term in the series expansion of the exponential adds a single bond, the quadratic term adds two single bonds, etc. The operator D promotes M_n to M_{n+1} as required when an extra bond is appended at the vertex, and the factor $M_1(\sigma)$ is the contribution of the free-hanging end of the added bond. The second step in the generation of rooted diagrams is the addition of a hypervertex of any of the permitted types $(\alpha,\beta,\cdots)$ to the free-hanging end of each of the single bonds. This is accomplished everywhere by replacing, in every exponential operator above,

$$M_1(\sigma)\rightarrow M_1(\sigma)-(\beta/N)DF_\alpha-(\beta/N)DF_\beta-\cdots.$$

[14] R. J. Riddel, Jr., and G. F. Uhlenbeck, J. Chem. Phys. **21**, 2056 (1953).

Single bonds can then be attached to each point, again with the replacement of all $M_n(\sigma)$ by $\exp[2\beta J_0 M_1(\sigma)D]\times M_n(\sigma)$. The indefinite continuation of this process leads to the generation of all rooted $\bar{S}$-reducible diagrams with a root of type α. The process can be closed by replacing every $M_n(\sigma)$ by $\exp[2\beta J_0\bar{M}_1(\sigma)D]M_n(\sigma)$, where, self-consistently,

$$\bar{M}_1(\sigma)=M_1(\sigma)-(\beta/N)D\bar{F}_\alpha-(\beta/N)D\bar{F}_\beta-\cdots, \quad (146)$$

and where $-(\beta/N)\bar{F}_\alpha$, $-(\beta/N)\bar{F}_\beta$, $\cdots$ are obtained from $-(\beta/N)F_\alpha$, $-(\beta/N)F_\beta$, $\cdots$ by replacing every $M_n(\sigma)$ in each by $\exp[2\beta J_0\bar{M}_1(\sigma)D]M_n(\sigma)$. The sum of all diagrams rooted in the α-type hypervertex is then $-(\beta/N)\bar{F}_\alpha$. Similarly, the sum of all diagrams rooted in the β-type hypervertex is $-(\beta/N)\bar{F}_\beta$. To obtain the sum of all *unrooted* diagrams we must, according to the procedure described previously, subtract from $-(\beta/N)\bar{F}_\alpha-(\beta/N)\bar{F}_\beta-(\beta/N)\bar{F}_\gamma-\cdots$ the sum of diagrams rooted in each type of hyperbond.

Generation of diagrams from a given type of hyperbond as root follows the above procedure closely. The contribution of an α-β type hyperbond is, for instance, $2\beta J_0[-(\beta/N)DF_\alpha][-(\beta/N)DF_\beta]$; the factor $2\beta J_0$ represents the bond itself, $-(\beta/N)DF_\alpha$ represents the hypervertex at one end, and $-(\beta/N)DF_\beta$ represents the hypervertex at the other end. To this root we can then adjoin single bonds, then hypervertices on the ends of these, and so on.

Rather than carrying out the calculation outlined above, the procedure can be aborted at the first step by choosing $\bar{S}$ so that the right-hand member of Eq. (146) vanishes. Physically, we choose $\bar{S}$ so that the sum of contributions of all hypervertices which can be affixed to a free bond end vanish. Then

$$M_1(\sigma)-(\beta/N)D\bar{F}_\alpha-(\beta/N)D\bar{F}_\beta+\cdots=0, \quad (147)$$

or, writing this in terms of the S_z variable,

$$\bar{S}=M_1(S_z)+(\beta/N)D\bar{F}_\alpha+(\beta/N)D\bar{F}_\beta+\cdots. \quad (148)$$

The bars on $\bar{F}_\alpha$ and $\bar{F}_\beta$ indicate that the value of $\bar{S}$ appearing within these quantities is that value determined self-consistently from Eq. (148), or that value for which $\bar{S}=\bar{M}_1(S_z)$ [compare Eqs. (148) and (146)]. With this choice of $\bar{S}$, the only nonvanishing diagrams are the hypervertices themselves, so that

$$-\beta F=-\beta F_0-\beta\bar{F}_\alpha-\beta\bar{F}_\beta+\cdots. \quad (149)$$

The above result can be seen alternatively in terms of the general procedure of subtraction of hyperbond-rooted diagrams from hypervertex-rooted diagrams. With the choice of $\bar{S}$ above, the hyperbond contributions sum to zero, since a bond can have the end $M_1(\sigma)$, or $-(\beta/N)D\bar{F}_\alpha$, or $-(\beta/N)D\bar{F}_\beta$, etc., which sum to zero by Eq. (147). The hypervertex-rooted diagrams give just $-(\beta/N)\bar{F}_\alpha$, $-(\beta/N)\bar{F}_\beta$, etc. Adding these contributions to the zero-order contribution, and multiplying by N to account for the possible positions of the root, we again obtain Eq. (149).

Two important points, which we now demonstrate, are the following. The choice of $\bar{S}$ in Eq. (148) minimizes the free energy (149). And the significance of $\bar{S}$ is that it is equal to the average value of S_z, as determined by Eq. (148).

That $\bar{S}$ minimizes the free energy follows from the fact that, when applied to the contribution of $\bar{S}$-irreducible diagrams [see Eq. (126)], D is equivalent to $(1/2\beta J_0)(\partial/\partial\bar{S})$, where D is the generating operator for the $M_n(S_z)$. Furthermore, $M_1(\sigma)=\bar{S}-M_1(S_z)$ is equal to $(1/2\beta J_0)(\beta/N)(\partial F_0/\partial\bar{S})$, where F_0 is the zero-order free energy [see Eq. (108)]. Hence, Eq. (148) can be rewritten as

$$0=\frac{1}{2\beta J_0 N}\left[\beta\frac{\partial F_0}{\partial\bar{S}}+\beta\frac{\partial\bar{F}_\alpha}{\partial\bar{S}}+\beta\frac{\partial\bar{F}_\beta}{\partial\bar{S}}+\cdots\right]$$

$$=\frac{1}{2\beta J_0 N}\frac{\partial(\beta F)}{\partial\bar{S}}. \quad (150)$$

Similarly, the fact that $\bar{S}$ is equal to the expectation value of S_z follows from the equivalence [see Eq. (125)] of the operator D to $(1/g\mu_0\beta)(\partial/\partial H)$, and from the identification of $M_1(S_z)$ as $(1/g\mu_0 N)(\partial F_0/\partial H)$. Hence Eq. (149) states

$$\bar{S}=\frac{1}{g\mu_0 N}\left[\frac{\partial F_0}{\partial H}+\frac{\partial\bar{F}_\alpha}{\partial H}+\frac{\partial\bar{F}_\beta}{\partial H}+\cdots\right] \quad (151)$$

$$=\frac{1}{g\mu_0 N}[\mathfrak{M}_0+\mathfrak{M}_\alpha+\mathfrak{M}_\beta+\cdots]. \quad (152)$$

To summarize, then, we can henceforth restrict our attention to $\bar{S}$-irreducible diagrams alone, with contribution $-\beta F$, providing that we impose the condition that $\partial F/\partial\bar{S}=0$, or alternatively and equivalently, that $g\mu_0 N\bar{S}$ is evaluated self-consistently as the magnetization.

The choice of $\bar{S}$ described above eliminates only $\bar{S}$-reducible diagrams; it does not eliminate all reducible diagrams. That this is an insufficient renormalization is corroborated in detail in Appendix C by computing the free energy to first order using only the $\bar{S}$ renormalization. Whereas the simple renormalization gave a divergent magnetization at the Curie temperature, the $\bar{S}$ renormalization leads to no Curie temperature at all. In order to obtain physically acceptable results it is necessary to eliminate all trees, carrying out the expansion in terms of the remaining irreducible diagrams (stars) only.

As an illustration of the diagrams which are not eliminated by the $\bar{S}$ renormalization we consider specifically the first-order contributions. The basic first-order diagram is the simple loop, and a full renormalization should leave only this diagram. We therefore consider all Cayley-Husimi trees, or all diagrams which can be made by interconnecting loops and chains of single bonds, excluding the possibility of

closing these chains. All such diagrams containing any single bonds are eliminated by the $\bar{S}$ renormalization, leaving clusters of loops, or Husimi trees. Unfortunately, we do not have another parameter such as $\bar{S}$ with which to eliminate these remaining reducible diagrams. We therefore do this by summing all ring diagrams which can be attached to a given vertex, incorporating this sum into the contribution of the vertex. This method of renormalization will be illustrated in detail in the following section.

From this point of view it is perhaps useful to characterize the $\bar{S}$ renormalization as a renormalization of *terminal* vertices, and the remaining renormalization as one of *internal* vertices. That is, if we start with a simple diagram composed of loop and bonds, we first reinterpret the terminal vertex so that its contribution implies the possibility of addition of a loop; this is the $\bar{S}$ renormalization, and we renormalize to zero, so that such diagrams vanish. In the remaining diagram we then select an internal vertex and reinterpret it so that it implies the possibility of adjoining all combinations of loops. We cannot renormalize to zero, so that the single loop diagram does remain. However each of its "vertices" now has a relatively complex meaning.

10. RENORMALIZATION: ELIMINATION OF REDUCIBLE DIAGRAMS TO FIRST ORDER

In Sec. 9, a procedure for the elimination of $\bar{S}$-reducible diagrams was exhibited. That renormalization was effected by an appropriate choice of the parameter $\bar{S}$. In this section we complete the elimination of all trees, making use of the method of subtraction of hyperbond-rooted diagrams from hypervertex-rooted diagrams, which was shown in the concluding portion of Appendix B to be applicable even to trees which are not $\bar{S}$-reducible. The discussion which follows will be specifically in terms of the renormalization of the first-order diagrams constructed of simple closed-loop stars; generalization to higher orders offers no special difficulties.

We designate as type α hypervertices all hypervertices which are Husimi trees (clusters of loops). Let $-\beta F_\alpha$ be the contribution of this type of hypervertex.

Consider now the class of diagrams consisting of type α hypervertices interconnected by open chains of simple bonds, i.e., what we have called Cayley-Husimi trees. All such diagrams, other than the particular diagrams consisting simply of a single type α hypervertex, are $\bar{S}$ reducible by definition and can be eliminated by choosing $\bar{S}$ as the self-consistent solution of

$$\frac{\partial(-\beta F_0)}{\partial \bar{S}}+\frac{\partial(-\beta F_\alpha)}{\partial \bar{S}}=0, \tag{153}$$

i.e.,

$$\bar{S}=\frac{-1}{Ng\mu_0}\left[-\frac{\partial F_0}{\partial H}-\frac{\partial F_\alpha}{\partial H}\right]=\frac{\mathfrak{M}_0+\mathfrak{M}_\alpha}{Ng\mu_0}. \tag{154}$$

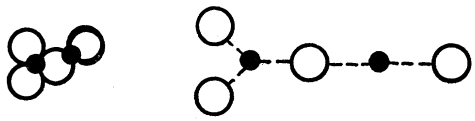

FIG. 4. Insertion of hypothetical dotted-line bonds to reduce $\bar{S}$-irreducible diagrams to analogs of $\bar{S}$-reducible diagrams.

The remaining diagrams consist only of single type α hypervertices; that is, of Husimi trees.

In Appendix B we have shown that the Husimi trees can be generated in a manner completely parallel to the $\bar{S}$-reducible diagrams. We introduce a construct there which makes it evident that these diagrams are topologically similar to the $\bar{S}$-reducible diagrams and further allows them to be described by the same terminology. The construct consists of "dotted line bonds" which schematically separate each articulation point from the various loops with which it is associated, as indicated in Fig. 4. These diagrams can now be described as consisting of simpler hyperbonds. In this case there are two types of hypervertices, the articulation points and the loops. There is a single type of hyperbond, for every dotted bond terminates in a simple vertex and in a loop (with a point removed). We shall now review the general discussion of the subtraction technique, as discussed in Sec. 9, for application to this class of diagrams.

To compute the free energy contribution $-\beta F_\alpha$ of the Husimi trees or loop clusters, the diagrams are generated first from each type of hypervertex regarded as a root; in this case a simple vertex root and a loop root. From the contributions of these hypervertex-rooted diagrams we subtract the contributions of the same set of diagrams generated from the hyperbond, as root; in this case the dotted-line bond.

Consider first the diagrams generated from a single vertex by connecting in turn one, two, three, . . . loops at the given point. Each of these diagrams has a distinguishable point, the root, and contributes a factor,

$$\Gamma=(1/2N)\textstyle\sum_{\mathbf{q}} 2\beta J(\mathbf{q})[1-2\beta J(\mathbf{q})M_2]^{-1}, \tag{155}$$

for every loop joined to that point. The root itself contributes M_2, M_4, M_6, . . . for one, two, three, . . . loops joined at the root. The contribution of these diagrams is exactly analogous to the series obtained for the zero-order diagrams in Eq. (A2). The contribution of these diagrams is thus

$$q_1^{(1)}=N\left(M_2\Gamma+\tfrac{1}{2}M_4\Gamma^2+\frac{1}{3!}M_6\Gamma^3+\cdots\right)$$

$$=N\sum_1^\infty\frac{1}{n!}\Gamma^n D_\Gamma{}^{2n}\phi, \tag{156}$$

where

$$\phi=\ln\sum_{-S}^{S}e^{\beta L S_z}, \tag{157}$$

and

$$D_\Gamma=\frac{1}{2\beta J_0}\left(\frac{\partial}{\partial\bar{S}}\right)_\Gamma; \tag{158}$$

D_Γ is an operator raising the order of a semi-invariant in precisely the same fashion as the operator D, except that the subscript denotes that Γ is to be regarded as constant when operating with D_Γ. Thus the series of Eq. (156) can be summed, giving

$$q_1^{(1)}=N[\exp(\Gamma D_\Gamma^2)-1]\phi. \tag{159}$$

The generation of all appropriate Husimi trees by successively including loops at each vertex of the above loops, etc., as we have seen in Sec. 9, is accomplished by merely replacing Γ by $\bar{\Gamma}$, where

$$\bar{\Gamma}=\frac{1}{2N}\sum_{\mathbf{q}}\frac{2\beta J(\mathbf{q})}{1-2\beta J(\mathbf{q})\bar{M}_2}=\Gamma(\bar{M}_2), \tag{160}$$

and where, self-consistently,

$$\bar{M}_2=\exp(\bar{\Gamma}D_\Gamma^2)M_2. \tag{161}$$

It is to be noted that the differentiation with differential operation D_Γ is now to be performed with constant $\bar{\Gamma}$. Thus we can also write (161) as

$$\bar{M}_2=D_\Gamma^2\exp(\bar{\Gamma}D_\Gamma^2)\phi=D_\Gamma^2\bar{\phi}, \tag{162}$$

where

$$\bar{\phi}=\exp(\bar{\Gamma}D_\Gamma^2)\phi. \tag{163}$$

Thus for the direct sum of diagrams generated from a point-root we obtain

$$\bar{q}_1=N[\exp(\bar{\Gamma}D_\Gamma^2)-1]\phi=N\bar{\phi}-N\phi. \tag{164}$$

The second direct sum, consisting of the contribution of diagrams generated from a loop-root, is obtained from the contribution of the loop-root itself by replacing M_2 by $\bar{M}_2$. Thus the second direct sum is

$$\bar{q}_2=-\tfrac{1}{2}\textstyle\sum_{\mathbf{q}}\ln[1-2\beta J(\mathbf{q})\bar{M}_2], \tag{165}$$

with $\bar{M}_2$ given by Eq. (161).

To obtain the compensating sum, we now generate diagrams from a dotted line bond-root. First we recall the contribution of the generator itself, before affixing additional loops. The contribution of loops with no points distinguishable is $\sum_{\mathbf{q}}\sum_n(1/2n)[2\beta J(\mathbf{q})M_2]^n$, as we saw in Eq. (119). When affixed to a dotted-line bond, one point of the loop is distinguishable, thereby eliminating the n-fold rotational symmetry, and giving as the contribution of the generator

$$\tfrac{1}{2}\sum_{\mathbf{q}}\sum_n[2\beta J(\mathbf{q})M_2]^n=\tfrac{1}{2}\sum_{\mathbf{q}}\frac{2\beta J(\mathbf{q})M_2}{1-2\beta J(\mathbf{q})M_2}=N\Gamma M_2.$$

Affixing all possible loops to this generator clearly is accomplished merely by replacing M_2 by $\bar{M}_2$ and Γ by $\bar{\Gamma}$. We thus find for the compensating sum,

$$\bar{q}_3=N\bar{M}_2\bar{\Gamma}. \tag{166}$$

Subtracting the compensating sum from the direct sums we obtain for $-\beta F_\alpha$,

$$-\beta F_\alpha=N\bar{\phi}-N\phi-\tfrac{1}{2}\textstyle\sum_{\mathbf{q}}\ln[1-2\beta J(\mathbf{q})\bar{M}_2]-N\bar{M}_2\bar{\Gamma}. \tag{167}$$

Adding $-\beta F_\alpha$ to $-\beta F_0=-\beta NJ_0\bar{S}^2+N\phi$ we obtain

$$-\beta\bar{F}_1=-\beta\bar{F}^{(0)}-\beta\bar{F}^{(1)}, \tag{168}$$

where

$$-\beta\bar{F}^{(0)}=-NJ_0\beta\bar{S}^2+N\bar{\phi}, \tag{169}$$

and

$$-\beta\bar{F}^{(1)}=-\tfrac{1}{2}\textstyle\sum_{\mathbf{q}}\ln[1-2\beta J(\mathbf{q})\bar{M}_2]-N\bar{M}_2\bar{\Gamma}. \tag{170}$$

Equation (169) represents the renormalized zero-order term, in which the renormalization consists of replacing ϕ by $\bar{\phi}$. Equation (170) represents the renormalized first-order term. In addition to replacing M_2 by $\bar{M}_2$, i.e., renormalizing the vertices, there is the additional term $-N\bar{\Gamma}\bar{M}_2$ in the free energy, arising from the dotted-line bond-rooted diagrams. In this term again M_2 is replaced by $\bar{M}_2$.

In Appendix D we obtain an integral representation for the renormalized semi-invariants. We find

$$\bar{M}_r(\beta L)=(2\pi)^{-\frac{1}{2}}\int_{-\infty}^{\infty}du\,M_r(\beta L-u(2\bar{\Gamma})^{\frac{1}{2}})\times\exp(-u^2/2), \tag{171}$$

$$\bar{\phi}(\beta L)=(2\pi)^{-\frac{1}{2}}\int_{-\infty}^{\infty}du\,\phi(\beta L-u(2\bar{\Gamma})^{\frac{1}{2}})\times\exp(-u^2/2). \tag{172}$$

Further,

$$\partial^s\bar{M}_r/\partial(\beta L)^s=\bar{M}_{r+s}, \tag{173}$$

while

$$\partial^t\bar{M}_r/\partial\bar{\Gamma}^t=\bar{M}_{r+2t}. \tag{174}$$

This renormalized form of the first-order free energy [Eqs. (168)–(172)] is our fundamental result. Along with the elimination of all reducible diagrams to first order we have maintained the convenient properties of $\bar{S}$; namely, that $\bar{S}$ be equal to the average value of S_z, and that this choice of $\bar{S}$ is the best choice in the sense that the free energy is a minimum with respect to $\bar{S}$. In the next section we shall examine some of the properties of our solution.

11. RESULTS AND DISCUSSION

From Eqs. (168)–(170) the free energy is

$$-\beta\bar{F}_1=-\beta NJ_0\bar{S}_1^2+N\bar{\phi}-\tfrac{1}{2}\textstyle\sum_{\mathbf{q}}\ln[1-2\beta J(\mathbf{q})\bar{M}_2]-N\bar{\Gamma}\bar{M}_2, \tag{175}$$

where

$$\bar{M}_r(\beta L)=(2\pi)^{-\frac{1}{2}}\int_{-\infty}^{\infty}du\,M_r(\beta L-u(2\bar{\Gamma})^{\frac{1}{2}})\times\exp(-u^2/2), \tag{176}$$

$$\bar{\phi}(\beta L)=(2\pi)^{-\frac{1}{2}}\int_{-\infty}^{\infty}du\exp(-u^2/2)\times\ln\sum_{-S}^{S}\exp\{[\beta L-u(2\bar{\Gamma})^{\frac{1}{2}}]S_z\}, \tag{177}$$

and where (175) is subject to the condition

$$\partial\bar{F}_1/\partial\bar{S}=0, \tag{178}$$

which is equivalent to

$$\bar{S}_1=(Ng\mu_0)^{-1}\partial\bar{F}_1/\partial H \quad \text{at constant } \beta \text{ and } \bar{S} \\ =\mathfrak{M}_1/Ng\mu_0. \tag{179}$$

The choice of $\bar{S}_1$ is associated with the elimination of the $\bar{S}$-reducible diagrams. The renormalization of the semi-invariants, as defined in Eqs. (176) and (177), is associated with the elimination of the remaining reducible diagrams to first order.

The first-order free energy is stationary with respect to functional variations in $\bar{\Gamma}$ at constant $\bar{S}$, β, and H, for

$$\partial(-\beta\bar{F}_1)/\partial\bar{\Gamma}=N[(\partial\bar{\phi}/\partial\bar{\Gamma})-\bar{M}_2]=0. \tag{180}$$

The fact that $-\beta\bar{F}_1$ is stationary with respect to both $\bar{S}$ and $\bar{\Gamma}$ is useful in the evaluation of $\bar{S}$ from Eq. (179)

$$\bar{S}_1=\frac{\mathfrak{M}_1}{Ng\mu_0}=\frac{1}{Ng\mu_0}\frac{\partial\bar{F}_1}{\partial H}=\bar{M}_1 \tag{181}$$

the derivatives $(\partial\bar{F}_1/\partial\bar{\Gamma})(\partial\bar{\Gamma}/\partial H)$ vanishing by Eq. (180), and similarly with respect to $(\partial\bar{F}_1/\partial\bar{S})(\partial\bar{S}/\partial H)$.

The internal energy is obtained again by differentiation at constant $\bar{S}$ and $\bar{\Gamma}$ [by virtue of Eqs. (178) and (180)], giving

$$\bar{E}_1/N=N^{-1}\partial(\beta\bar{F}_1)/\partial\beta, \quad (H,\ \bar{\Gamma} \text{ and } \bar{S} \text{ constant}) \tag{182}$$

$$=J_0\bar{S}_1^2-[2J_0\bar{S}_1+g\mu_0H]\bar{M}_1 \\ -\bar{\Gamma}\bar{M}_2/\beta+\bar{\Gamma}\bar{M}_3-\bar{\Gamma}\bar{M}_3 \tag{183}$$

$$=-\Big[J_0\bar{S}_1^2+g\mu_0H\bar{S}_1 \\ +\frac{1}{2N\beta}\sum_{\mathbf{q}}\frac{2\beta J(\mathbf{q})\bar{M}_2}{1-2\beta J(\mathbf{q})\bar{M}_2}\Big]. \tag{184}$$

The first of these terms has exactly the form of the molecular field result (with, of course, a different value of $\bar{S}$). The second term is readily recognized as the sum of (renormalized) simple loop diagrams. This latter term represents the effect of short-range spin-spin correlations, absent in the molecular field result.

The susceptibility is

$$\chi=N^{-1}\partial\mathfrak{M}_1/\partial H=g\mu_0\partial\bar{S}_1/\partial H. \tag{185}$$

In Appendix E we have evaluated $\partial\bar{S}/\partial H$ and from Eq. (E7) we have

$$\chi=\beta g^2\mu_0^2\frac{\bar{M}_2+\bar{\Delta}\bar{M}_3^2/(1-\bar{\Delta}\bar{M}_4)}{1-2\beta J_0[\bar{M}_2+\bar{\Delta}\bar{M}_3^2/(1-\bar{\Delta}\bar{M}_4)]}. \tag{186}$$

In order to study the above results it is convenient to express $\bar{\Gamma}$ and $\bar{\Delta}$ in terms of a function $F(x)$ which has been studied by Lax[15] in connection with the spherical model. Defining $F(x)$ by

$$F(x)=(1/N)\textstyle\sum_{\mathbf{q}}[x-J(\mathbf{q})/J_0]^{-1}, \tag{187}$$

then if

$$x=(2\beta J_0\bar{M}_2)^{-1} \tag{188}$$

we have

$$\bar{\Gamma}=\beta J_0[x^2F(x)-x], \tag{189}$$

and

$$\bar{\Delta}=\frac{1}{2N}\sum_{\mathbf{q}}\left(\frac{2\beta J(\mathbf{q})}{1-2\beta J(\mathbf{q})\bar{M}_2}\right)^2 \\ =\frac{-1}{2\bar{M}_2{}^2}[x^2F'(x)+2xF(x)-1]. \tag{190}$$

The properties of $F(x)$ for three-dimensional lattices with nearest-neighbor interactions have been shown to be as follows. $F(x)$ has some finite value (of the order of unity) at $x=1$, and decreases monotonically for values of x greater than one, behaving as const/x for sufficiently large x. For $x>1$, but in the vicinity of $x=1$, $F(x)$ has the approximate form $F(x)=F(1)-0.8(x-1)^{\frac{1}{2}}$, the coefficient 0.8 varying slightly from lattice to lattice. Thus $F(x)$ has a negatively infinite slope to the right of $x=1$. Furthermore, $F(x)$ diverges for $x<1$, and this region of the variables is not physically acceptable. It should be noted that $\bar{\Gamma}$ is well behaved as $x\to 1$ (from above), whereas $\bar{\Delta}$ diverges as $x\to 1$.

With these results we are able to investigate the behavior of χ, and in particular to evaluate the Curie temperature. The Curie temperature is the temperature at which χ diverges (for $H=0$) and is therefore determined by the condition

$$1-2\beta_cJ_0\bar{M}_2-2\beta_cJ_0\bar{\Delta}\bar{M}_3^2/(1-\bar{\Delta}\bar{M}_4)=0. \tag{191}$$

We see that a solution of the equation is obtained from

$$1-2\beta_cJ_0\bar{M}_2=0, \tag{192}$$

or

$$x_c=1. \tag{193}$$

That this is so follows from the fact that $\bar{\Delta}$ diverges at $x=1$, so that the third term in Eq. (191) reduces simply to $\bar{M}_3^2/\bar{M}_4$. This ratio, in turn, vanishes at the Curie temperature because all odd semi-invariants involve averages of odd powers of S_z and therefore vanish at T_c, whereas even semi-invariants do not.

In order to compare our results with other investigations we specifically study the case of spin $\frac{1}{2}$ and nearest-neighbor interactions in face-centered, body-centered, and simple cubic lattices.

$$M_1(x)=\tfrac{1}{2}\tanh(\tfrac{1}{2}x), \tag{194}$$

$$M_2(x)=DM_1(x)=\tfrac{1}{4}\operatorname{sech}^2(\tfrac{1}{2}x), \tag{195}$$

$$M_3(x)=-2M_2M_1. \tag{196}$$

Using the integral form of $\bar{M}_2$ particularized to spin

[15] M. Lax, Phys. Rev. **97**, 629 (1955).

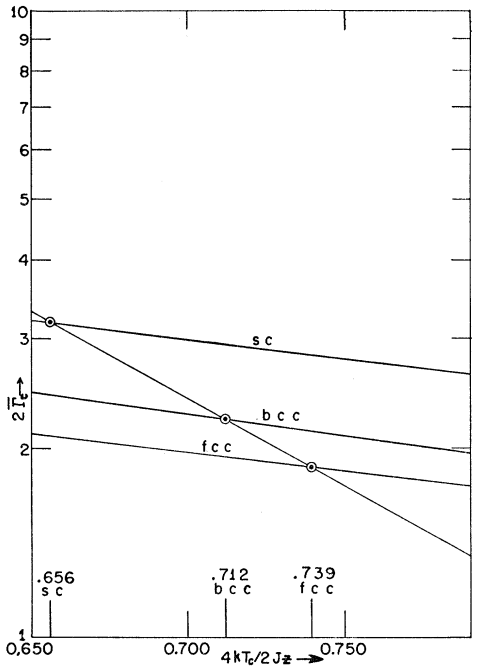

FIG. 5. Determination of critical temperature by graphical solution of Eqs. (197) and (199).

$\frac{1}{2}$, we obtain for Eq. (192),

$$t\equiv\frac{4kT_c}{2Jz}=(2\pi)^{-\frac{1}{2}}\int_{-\infty}^{\infty}du\,\exp(-u^2/2)\times\operatorname{sech}^2[u(2\bar{\Gamma})^{\frac{1}{2}}/2]. \quad (197)$$

We have evaluated this integral numerically as a function of $\bar{\Gamma}_c$ and plotted the result in Fig. 5. $\bar{\Gamma}_c$ is, however, itself a function of t, since

$$\bar{\Gamma}_c=\beta J_0[x^2F(x)-x]=(1/t)2[F(1)-1]. \quad (198)$$

$F(1)$ has been evaluated for the three lattices considered, for nearest-neighbor interactions, by Watson.[16] He obtained the values $F(1)=1.51638$ for simple cubic, $F(1)=1.39320$ for bcc, and $F(1)=1.34466$ for fcc lattices.

In Fig. 5 we also plot t versus $\bar{\Gamma}_c$ for each lattice from the equation

$$t=2[F(1)-1]/\bar{\Gamma}_c. \quad (199)$$

The intersection is the simultaneous solution of the two equations, (197) and (199), and gives T_c for each type of lattice. Comparison of these critical temperatures with the results of other theories is presented in Table I.

It will be noted that our results for T_c are in rather close agreement with the results of the spherical model, and with the estimates of Trefftz.[5] Her values were obtained by extrapolation of graphs of the reciprocal of the specific heat obtained from exact series expansion at high and low temperatures.

[16] G. N. Watson, Quart. J. Math. **10**, 266 (1939).

The specific heat is given by

$$c_V/k=\frac{1}{Nk}\frac{\partial\bar{E}_1}{\partial T}=\beta^2\frac{\partial}{\partial\beta}[J_0\bar{S}_1^2+g\mu_0H\bar{S}_1+\beta^{-1}\bar{\Gamma}\bar{M}_2] \quad (200)$$

$$=\beta[2J_0\bar{S}_1+g\mu_0H]\left[\beta\frac{\partial\bar{S}_1}{\partial\beta}+\bar{\Gamma}\beta\frac{\partial\bar{M}_2}{\partial\beta}+\bar{M}_2\beta\frac{\partial\bar{\Gamma}}{\partial\beta}-\bar{\Gamma}\bar{M}_2\right] \quad (201)$$

$$=[\beta L+2\beta J_0\bar{\Gamma}\bar{M}_3]\beta\frac{\partial\bar{S}_1}{\partial\beta}+[\bar{M}_2+\bar{M}_4\bar{\Gamma}]\beta\frac{\partial\bar{\Gamma}}{\partial\beta}+[\beta L\bar{M}_3-\bar{M}_2]\bar{\Gamma}. \quad (202)$$

The behavior of this, and similar quantities, in the vicinity of the transition temperature is studied in Appendix F. It is shown there that the specific heat is continuous at T_c with an infinite slope on the low-temperature side and with a finite slope on the high-temperature side.[17]

The expression (192) for T_c is of interest in reconsidering the validity of the $1/z$ classification of diagrams, either as applied by us to irreducible linked diagrams or as applied to unrenormalized diagrams. For definiteness, consider simple loops. If the loops are renormalized, each bond contributes a factor $2\beta J_{ij}\bar{M}_2$, and Eq. (192) for the Curie temperature shows that this quantity is of order $1/z$. If there are n bonds in the loop we have n such factors, and $(n-1)$ summations, each of which gives a factor z. Hence the diagram is of order $1/z$, as we assumed. If the loops are unrenormalized, however, each bond instead contributes a factor $2\beta J_{ij}M_2$ and hence the diagram is of order $(M_2/\bar{M}_2)^n(1/z)$. As $\bar{M}_2$ deviates significantly from M_2, the ratio $(M_2/\bar{M}_2)^n$ becomes enormously large for large n (large diagrams),

TABLE I. Approximations to the Curie temperature.

	Simple cubic	Body-centered cubic	Face-centered cubic
Molecular field[a]	1	1	1
Bethe[b] and quasi-chemical	0.822	0.864	0.914
Rushbrooke[c] and Scoins	0.794	0.835	0.882
Kikuchi[d] (2nd approximation)	0.768	0.869	0.835
Low-temperature[e] series	0.748	0.784	0.805
High-temperature[f] series	0.752	0.794	0.816
Spherical model[b]	0.660	0.718	0.740
Trefftz[g]	0.665	0.704	0.718
Our calculation	0.656	0.712	0.739

[a] See reference 6.
[b] See reference 7.
[c] G. S. Rushbrooke and I. Scoins, Proc. Roy. Soc. (London) **A230**, 74 (1955).
[d] See reference 8.
[e] See reference 3.
[f] C. Domb and M. F. Sykes, Proc. Roy. Soc. (London) **A240**, 214 (1957).
[g] See reference 5.

[17] For comparison with the specific heat of the spherical model see reference 9.

totally dominating the factor $1/z$ and vitiating the basis of the classification of unrenormalized diagrams.

The agreement of our results with the rigorous high-temperature series is evident, thereby providing an independent justification for the selection of the loop diagrams. Each bond in a diagram is associated with a factor β, and the first-order term in β is contributed by a single bond, the second-order term by the summation of all diagrams with two bonds, etc. Our first-order expansion contains all diagrams with one and two bonds, omits only the diagram (3,1) (Fig. 1) of all those with three bonds, and only the diagrams (4,1), (4,2), and (4,4) of the twelve types of diagrams with four bonds, and since odd semi-invariants vanish at the Curie temperature and above, the only one of these omitted diagrams which makes a nonzero contribution in the high-temperature region is the quadruple bond (4,1). Furthermore such omitted diagrams probably contribute the smallest contributions because they involve the highest-ordered semi-invariants. Consequently, the first-order results agree exactly with the high temperature results to the coefficient of T^{-3}, and the coefficient of T^{-4} is approximately correct. It would be quite easy to add the missing four-bond diagram, and, in fact, our method provides a technique for carrying out a rigorous high-temperature expansion which is much simpler than the conventional Kirkwood method.[18]

Finally, our results agree with the rigorous low-temperature results—and in the ferromagnetic case, in fact, reduces to the spin-wave result, as we shall see in a separate paper. This again justifies the choice of renormalized loop diagrams in the low temperature region. An *a priori* rather than an *a posteriori* justification apparently could be based on the behavior of the semi-invariants considered as functions of their order. The second semi-invariant $M_2(S_z)$ is the mean square of $(S_z-\bar{S})$ and the third semi-invariant $M_3(S_z)$ is the mean third power of $(S_z-\bar{S})$, although higher semi-invariants do not maintain this simple form. Nevertheless, it is plausible that the values of the semi-invariants decrease rapidly with increasing order. Particularly in the low-temperature region this suggests a classification of diagrams according to the order of the associated semi-invariants. The closed-loop diagrams which we have summed are just those which involve no renormalized semi-invariants of higher than second order.

In conclusion, then, we have given a theory which, to first order, agrees with the rigorous low-temperature and high-temperature results, which agrees well with the best estimates in the Curie temperature regions, and which is justified by plausible and self-consistent criteria, in each temperature region, for the choice of diagrams.

Note added in proof. M. Coopersmith has informed us of his discovery that the spontaneous magnetization of the spherical model becomes zero at two distinct temperatures, one corresponding to the conventional Curie temperature at which the susceptibility diverges, and a second temperature at which the magnetization is discontinuous. The conventional solution is formally unstable. Our model exhibits similar properties. Englert and Brout have suggested the following diagrammatic interpretation. The susceptibility is obtained by differentiating the free energy twice—each such differentiation effectively rooting a point. By rooting two points the differentiations effectively introduce cross-link bonds, and thereby inconsistently introduce $1/z^2$ diagrams in the expression for χ. Englert points out that elimination of these spurious diagrams can be effected simply by holding $\beta^{-1}\bar{\Gamma}$ constant in the differentiations with respect to H or β, or equivalently, by setting $\bar{\Delta}=0$ in our result. The Curie temperature is unaffected, but the specific heat is then discontinuous (and nonzero above the Curie temperature). A detailed discussion of this problem will be given elsewhere by Englert.

APPENDIX A. DIRECT SUMMATION OF ZERO-ORDER DIAGRAMS

In this Appendix the zero-order diagrams are summed directly, thereby giving the zero-order free energy; we thereby illustrate the equivalence of the direct summation to the alternative procedure of elimination of diagrams by an appropriate choice of $\bar{S}$.

A second important point illustrated is the use of a compensating summation technique whereby diagrams are summed by first summing several classes of rooted diagrams and subtracting certain classes from others.

The zero-order diagrams consist of open chains, which may be forked in complex ways. A diagram having n bonds has $(n+1)$ vertices. Consider some particular zero-order diagram, such as Fig. 6(a), which has 6 bonds and 7 vertices. There are two sets of equivalent vertices; the vertices 1, 2, and 3, and the vertices 6 and 7. Each such set of r equivalent vertices contributes a factor $1/r!$ to the weight factor of the diagram. Suppose we now add some structure to the diagram, joining it in every possible way to one or

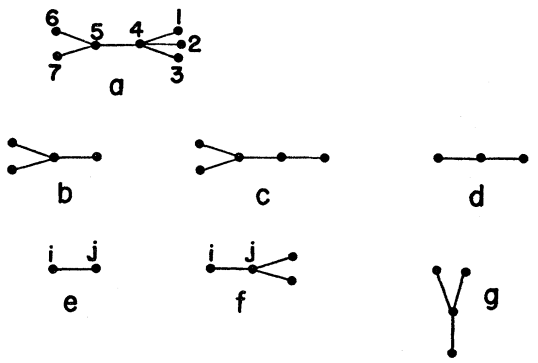

FIG. 6. Generation of Cayley trees.

[18] D. ter Haar, *Elements of Statistical Mechanics* (Rinehart and Company, New York, 1956).

more of the equivalent vertices; let us say to the vertices 1, 2, and 3. Furthermore, let the contribution of this added structure when formed be A, this quantity including a product of exchange integrals, internal weight factors, and spin factors (semi-invariants). The result of adding these structures is to change the factors $M_1^3/3!$ which occurred in the initial diagram to

$$(1/3!)M_1^3 \rightarrow (1/3!)(M_1+A)^3 = (1/3!)(M_1^3+3M_1^2A+3M_1A^2+A^3). \quad \text{(A1)}$$

The four terms on the right correspond to the following four ways of adding the structure A. The first term involves the addition of no new structures. The second term involves the addition of one new structure; this leaves only two equivalent vertices and changes the proper weight factor from $(1/3!)$ to $(1/2!)=(3/3!)$. The third term involves the addition of two new structures; these are equivalent, and again the proper weight factor is $1/2!$. Finally, the fourth term corresponds to the possibility of adding the structure A to each of the three vertices.

According to the above procedure, to join structures A to r-fold equivalent vertices one merely replaces M_1^r by $(M_1+A)^r$, and this properly accounts for the changes in the multiplicities.

We fix our attention on a particular vertex, to which we adjoin bonds, in turn adjoining new bonds to those, and thus sequentially building up all possible diagrams. We shall find that certain diagrams are counted multiply, because they can be built up in different ways. However, we first ignore this fact and sum the sequentially built diagrams directly. We shall then demonstrate the procedure for correcting for the multiple counting in the summation.

Consider the sequence of attaching one, two, three, . . . bonds to a particular vertex. The contribution of this sequence of diagrams is

$$T^{(0)}=\sum_{n=1}^{\infty} t_n{}^{(0)}=\sum_{n=1}^{\infty} M_n(\sigma)\frac{[2\beta J_0 M_1(\sigma)]^n}{n!}, \quad \text{(A2)}$$

or, by virtue of Eqs. (20) and (21),

$$T^{(0)}=\ln\langle\exp[2\beta J_0 M_1(\sigma)\sigma]\rangle. \quad \text{(A3)}$$

Now consider the particular diagram with three bonds, which is responsible for the contribution $t_3{}^{(0)}$ in Eq. (A2). To each of the free ends we can affix one, two, three, . . . bonds in turn. As we have seen, the effect of these additions is

$$t_3{}^{(0)}=\frac{1}{3!}M_3(2\beta J_0 M_1)^3 \rightarrow \frac{1}{3!}M_3(2\beta J_0)^3 \times\Big[M_1+M_2(2\beta J_0 M_1)+\frac{1}{2!}M_3(2\beta J_0 M_1)^2 +\cdots+\frac{1}{n!}M_{n+1}(2\beta J_0 M_1)^n+\cdots\Big]^3, \quad \text{(A4)}$$

or

$$t_3{}^{(0)} \rightarrow t_3{}^{(1)}=\frac{1}{3!}M_3(2\beta J_0\Sigma^{(1)})^3, \quad \text{(A5)}$$

where

$$\Sigma^{(1)}=\sum_{n=0}^{\infty}\frac{1}{n!}M_{n+1}(2\beta J_0 M_1)^n \quad \text{(A6)}$$

$$=\frac{\partial}{\partial(2\beta J_0 M_1)}\sum_{n=0}^{\infty}\frac{1}{(n+1)!}M_{n+1}(2\beta J_0 M_1)^{n+1} \quad \text{(A7)}$$

$$=\frac{\partial}{\partial(2\beta J_0 M_1)}\ln\langle\exp(2\beta J_0 M_1\sigma)\rangle \quad \text{(A8)}$$

$$=\langle\sigma\exp(2\beta J_0 M_1\sigma)\rangle/\langle\exp(2\beta J_0 M_1\sigma)\rangle \quad \text{(A9)}$$

$$=\bar{S}-M_1{}^{(1)}(S_z), \quad \text{(A10)}$$

and where

$$M_1{}^{(1)}(S_z)=\frac{\langle S_z\exp(2\beta J_0 M_1\sigma)\rangle}{\langle\exp(2\beta J_0 M_1\sigma)\rangle} =(\sum_{-S}^{S} S_z\exp\{[2\beta J_0 M_1(S_z)+g\mu_0\beta H]S_z\})/ (\sum_{-S}^{S}\exp\{[2\beta J_0 M_1(S_z)+g\mu_0\beta H]S_z\}). \quad \text{(A11)}$$

To summarize: adding bonds to the vertices of the diagram $t_3{}^{(0)}$ merely replaces $M_1(\sigma)$ by $\Sigma^{(1)}$ [Eq. (A5)]. The quantity $\Sigma^{(1)}$ has precisely the same form as $M_1(\sigma)$ [Eq. (A10)], except that in the density function the quantity $\bar{S}$ is replaced by $M_1(S_z)$ [Eq. (A11)].

If the process above is carried out for every diagram represented in Eq. (A2), we obtain

$$T^{(1)}=\sum_{n=1}^{\infty}\frac{1}{n!}M_n(\sigma)(2\beta J_0\Sigma^{(1)})^n =\ln\langle\exp(2\beta J_0\Sigma^{(1)}\sigma)\rangle. \quad \text{(A12)}$$

Adding another shell of bonds to each of these diagrams, we find

$$T^{(2)}=\ln\langle\exp(2\beta J_0\Sigma^{(2)}\sigma)\rangle, \quad \text{(A13)}$$

where

$$\Sigma^{(2)}=\bar{S}-M_1{}^{(2)}(S_z), \quad \text{(A14)}$$

and where $M_1{}^{(2)}(S_z)$ has the form of $M_1{}^{(1)}(S_z)$ with $M_1(S_z)$ replaced by $M_1{}^{(1)}(S_z)$ in the exponential weighting factors,

$$M_1{}^{(2)}(S_z)=(\sum_{-S}^{S} S_z\exp\{[2\beta J_0 M_1{}^{(1)}(S_z)+g\mu_0\beta H]S_z\})/ (\sum_{-S}^{S}\exp\{[2\beta J_0 M_1{}^{(1)}(S_z)+g\mu_0\beta H]S_z\}). \quad \text{(A15)}$$

Continuing, we find

$$T^{(n)}=\ln\langle\exp(2\beta J_0\Sigma^{(n)}\sigma)\rangle, \tag{A16}$$

where

$$\Sigma^{(n)}=\bar{S}-M_1{}^{(n)}(S_z), \tag{A17}$$

and

$$M_1{}^{(n)}(S_z)=(\sum_{-S}^{S}S_z\exp\{[2\beta J_0M_1{}^{(n-1)}(S_z)+g\mu_0\beta H]S_z\})/$$
$$(\sum_{-S}^{S}\exp\{[2\beta J_0M_1{}^{(n-1)}(S_z)+g\mu_0\beta H]S_z\}). \tag{A18}$$

In the limit, as $n\rightarrow\infty$, we equate $M_1{}^{(n)}(S_z)$ to $M_1{}^{(n-1)}(S_z)$ and denoting the limiting value by

$$\bar{M}_1(S_z)=(\sum_{-S}^{S}S_z\exp\{[2\beta J_0\bar{M}_1(S_z)+g\mu_0\beta H]S_z\})/$$
$$(\sum_{-S}^{S}\exp\{[2\beta J_0\bar{M}_1(S_z)+g\mu_0\beta H]S_z\})$$
$$=SB_s[2\beta J_0\bar{M}_1(S_z)S+g\mu_0\beta HS], \tag{A19}$$

where, as in Eq. (97), B_s is the Brillouin function. The correspondence with the zero-order result of Sec. 7 begins to emerge, the quantity $\bar{M}_1(S_z)$ being identical to the quantity $\bar{S}_0$ there introduced.

The limiting value of $T^{(n)}$ is obtained by replacing $M_1{}^{(n)}(S_z)$ by $\bar{M}_1(S_z)$ in Eqs. (A17) and (A16):

$$T=\ln\langle\exp\{2\beta J_0[\bar{S}-\bar{M}_1(S_z)]\sigma\}\rangle. \tag{A20}$$

However, this quantity is not the proper contribution to the free energy, because certain diagrams have been multiply counted. For instance, adding one bond to Fig. 6(b) produces Fig. 6(c). Also, adding one fork to Fig. 6(d) produces Fig. 6(c). In our counting we have permitted both of these possibilities, so that the latter diagram has been multiply counted.

In the above procedure, we have arbitrarily singled out one particular vertex as the generating center of all diagrams. By making this vertex unique we have destroyed the symmetry of some diagrams, attributing to them incorrect weight factors. Thus suppose our initial vertex is labeled i in Fig. 6(e). Adding a fork to j we obtain Fig. 6(f), and we have attributed the weight factor $\frac{1}{2}$ to this diagram. Clearly, it has a threefold symmetry, but that symmetry was reduced by singling out the origin vertex i as a root. In terms of the expansion having no distinguishable points, the rooted diagram gives the wrong contribution unless j rather than i is the root.

Let us consider an alternate way of generating diagrams. We fix our attention on a particular bond as root, rather than a particular vertex. This bond alone gives a contribution

$$R^{(0)}=(1/2!)(2\beta J_0)M_1{}^2(\sigma), \tag{A21}$$

Adding all possible bonds precisely as we have done above again simply replaces $M_1(\sigma)$ by $\bar{S}-\bar{M}_1(S_z)$ so that the sum of all diagrams generated by a unique bond is

$$R=(1/2!)(2\beta J_0)[\bar{S}-\bar{M}_1(S_z)]^2. \tag{A22}$$

Again, various diagrams have been incorrectly counted. However, we now show that by subtracting R from T we cancel all counting errors and obtain the correct contribution to zero order.

Consider some diagram such as Fig. 6(g). In generating from a unique point, this diagram can be built with the central vertex as the root, and it then carries the correct symmetry factor. But it can also be built with one of the other vertices as roots, and it then carries an incorrect symmetry factor. Both of these possibilities are included in T. In generating from a bond, the diagram has the same (incorrect) symmetry factor as it has in building from an outer vertex. Hence in the difference $T-R$, only the contribution arising from the central vertex root remains, and it carries the correct symmetry factor.

For every Cayley tree a similar pairing of bonds and vertices is possible, so that in the difference $T-R$ only the contribution from certain central elements remain. The basis of this pairing of vertices and bonds lies in the concept of the central element of a diagram.

It is a well-established theorem[19] that every Cayley tree has either a central vertex or a central bond, defined as follows. One severs the diagram at the articulation point closest to each extremity of the diagram, thereby removing every bond with only a single articulation point (i.e., every terminal bond). One then repeats the process with the residual diagram, again removing each terminal bond. After repeating this procedure a certain number of times (this number is called the order of reducibility of the diagram), only a single vertex or a single bond (with its two associated vertices) remains. This remaining vertex or bond is called the center of the diagram.

At each step in the reduction of a diagram, the removal of a terminal bond also removes the terminal vertex. The bond and vertex which are thus removed together clearly have the property that in the original diagram rooting one or rooting the other changes the symmetry of the diagram in the same way. The diagram rooted at such a vertex and the diagram rooted at such a bond cancel in the difference $T-R$.

Rooting the central element of a diagram does not change the symmetry of the diagram. This is almost self-evident, for rooting the diagram at an element merely makes that element unique and distinguishable. But the central element is already unique and distinguishable, so that rooting it does not alter the diagram symmetry.

The considerations above are essentially a proof of the subtraction procedure. In the first and simplest case, in which the diagram of interest has a central vertex, then all contributions cancel in $T-R$ except

[19] M. S. Green, J. Math. Phys. **1**, 391 (1960).

that generated from the central vertex as root, and that contribution carries the correct symmetry factor. If the central element is a bond, however, we must consider two cases. Let us suppose that the two vertices at the ends of this bond were nonequivalent in the original diagram. Then each of these vertices contributes the given diagram to T, and each with the correct symmetry factor. The bond itself, as a root, contributes the diagram once to R, again with the correct symmetry factor. Thus the diagram remains correctly in the difference $T-R$. The remaining case is that in which the two vertices at the ends of the central bond were equivalent in the original diagram; this implies a twofold reflection symmetry in the original diagram, as in (5,10) of Fig. 1. Then we generate the diagram from one of these vertices in T (only from one of the vertices, because we use every *type* of vertex once as root). But in rooting such a vertex the diagram loses its reflection symmetry and hence has a symmetry factor twice as large as it should. From this we subtract (in R) the bond-rooted diagram, with the correct symmetry factor. Again the difference $T-R$ is correct.

Accordingly, we obtain the zero-order free energy by writing

$$-\beta F^{(0)}=-\beta F_0+N(T-R), \tag{A23}$$

where F_0 is given in Eq. (15). We thus find

$$-\beta F^{(0)}=-\tfrac{1}{2}N(2\beta J_0)\bar{M}_1{}^2(S_z)$$
$$+N\ln\sum_{-S}^{S}\exp\{[2\beta J_0\bar{M}_1(S_z)+g\mu_0\beta H]S_z\}, \tag{A24}$$

which is identical with Eq. (98), in virtue of the identity of $\bar{M}_1(S_z)$ and S_0. Thus we corroborate that the renormalization process of Sec. 7 is completely equivalent to the direct summation procedure, utilizing the method of subtraction of rooted diagrams as developed above.

The zero-order diagrams have been summed by the expedient of subtracting the contribution of all diagrams generated from a unique bond root from the contributions of all diagrams generated from a unique vertex root. In Appendix B a topological analysis of these and related higher order diagrams leads to the conclusion that it is always possible to generate diagrams from various roots regarded as unique, and that by appropriate subtraction of the resulting contributions all unrooted diagrams can be counted correctly.

APPENDIX B. SUMMABILITY OF $\bar{S}$-REDUCIBLE DIAGRAMS

In this Appendix we extend the method of summability by subtraction of rooted diagrams, established for the zero-order diagrams in Appendix A, to a more general class of diagrams.

It was shown in Appendix A that the zero-order diagrams could be generated and summed as follows. One first chooses a vertex as a root. To this vertex root one adds bonds in various ways, in turn adding bonds to these bonds, and thereby successively ramifying the structure to obtain all possible zero-order diagrams. Rooting the diagrams simplifies the calculation of the effect of adding successive structures, but leads to two types of errors. The symmetry factors so obtained are incorrect, and diagrams are multiply counted. Each of these errors is compensated for by repeating the process, starting from a unique bond-root, rather than from a unique vertex-root. The difference in the contributions so calculated gives the proper contribution of the zero-order diagrams.

The diagrams to which we first wish to extend the above method of summation are the "$\bar{S}$-reducible diagrams," defined as diagrams having a single bond joined to an articulation point. Further generalization to all trees will be made subsequently.

It is clear that any $\bar{S}$-reducible diagrams can be considered as composed of $\bar{S}$-irreducible diagrams connected together by single-bond chains. To suggest a relationship of $\bar{S}$-reducible diagrams to Cayley trees it is useful to refer to these $\bar{S}$-irreducible substructures as "hypervertices" and, for our present purposes, to think of them merely as different varieties of points, strung on single-bond chains. It is useful also to think of the single bonds as "hyperbonds" of several varieties, determined by the nature of their two associated vertices (or hypervertices).

As discussed in Sec. 9, all $\bar{S}$-irreducible substructures can be considered as hypervertices, so that $\bar{S}$-reducible trees become analogous to Cayley trees.

Each $\bar{S}$-reducible tree has either a central bond or a central hypervertex, defined by a straightforward generalization of the reduction procedure described for Cayley trees in Appendix A.

Each step of reduction removes, from each branch, a single bond along with its external hypervertex. Furthermore, the symmetry of the diagram is identical if either this bond or this hypervertex is considered as root. That is, the contribution calculated for the diagram if generated from that hypervertex as root is identical to the contribution generated from that bond as root.

Consider the class of diagrams that is composed of all possible interconnections (by single-bond chains) of a particular set of types of hypervertices. We could attempt to calculate the contribution of this class of diagrams by generating the diagrams from a distinguishable hypervertex of any type. Or we could calculate the contribution by generating the diagrams from each type of hyperbond as root. If the sum of the contributions calculated on the basis of each type of hyperbond as root is subtracted from the sum calculated on the basis of each type of hypervertex as root, all contributions except those arising from the central root of the diagram will vanish.

If the center of a diagram is a hypervertex, it is clear

that the above subtraction procedure leads to the correct summation of diagrams.

If the center of a diagram is a hyperbond, the net contribution after the subtraction procedure consists of the contributions generated from the hypervertices at the ends of the bond, minus the contribution generated from the single bond itself. We consider two cases; either the two hypervertices are of the same type, or they are of different types. In the former case the hypervertices generate the diagram with a spurious factor of two, arising from the fact that the true symmetry of the center should contribute a factor of one-half because of the reflection symmetry, but that this symmetry is destroyed if one of the equivalent hypervertices is considered as unique. The central bond generates the diagrams properly, and the subtraction procedure therefore again leads to the correct summation. In the second case, the two hypervertices at the ends of the central bond are different. In this case, each of the hypervertices generate the diagrams with correct symmetry factors, as does the central bond itself. In the subtraction the bond-rooted diagrams cancel the hypervertex rooted diagrams of one hypervertex, leaving those of the other hypervertex root.

To repeat then, we have shown that all $\bar{S}$-reducible diagrams are summable as follows. Each type of $\bar{S}$-irreducible substructure is considered as a "hypervertex" and used as a root for the generation and summation of the diagrams. Similarly, each type of hyperbond (a simple bond terminated by particular types of hypervertices) is used as a root. If the sum of hyperbond-rooted contributions is subtracted from the sum of hypervertex-rooted contributions, the resulting difference is the correct summation of the diagrams. This is the result required for Sec. 9.

The generalization of this subtraction procedure to more complicated trees which are not $\bar{S}$-reducible, is straightforward. For any such tree every articulation point is a junction of two or more stars. In order to make clear the direct applicability of our previous discussion to this case, we make the following construct. At each articulation point we indicate the connection of each star to the articulation point by a hypothetical dotted-line bond, as in Fig. 4. Such dotted-line bonds make no contribution to the free energy, of course, but serve to reduce the topology of these $\bar{S}$-irreducible diagrams to that of the $\bar{S}$-reducible diagrams already considered. The analysis applied above to the $\bar{S}$-reducible diagrams is then clearly applicable to trees that are not $\bar{S}$-reducible. The hypervertices in this case are either the articulation points or one of a set of stars. The hyperbonds comprise the dotted-line bonds, which now always join one simple vertex to a star.

Consider finally the class of trees composed of interconnections of a particular set of types of stars. These diagrams can be generated from a distinguishable star of each type (excluding single bonds) as root, leading to a set of contributions. Or, alternatively, these diagrams can be generated from the distinguishable hyperbonds and dotted-line hyperbonds as roots. Subtracting the latter sums from the former sums then gives the correct contribution for all diagrams. Thus we find that we can sum all trees by this subtraction procedure, and we shall consider all trees as reducible diagrams, all stars as irreducible diagrams.

APPENDIX C. A SIMPLE BUT ASYMMETRICAL RENORMALIZATION PROCEDURE

In Sec. 10 we develop the theory of symmetric renormalization of all vertices. A simpler procedure, described briefly in Sec. 9, is simply to renormalize open end-vertices, as done in zero order. We show that such a procedure results in $\bar{S}$ being equal to the magnetization, and in the free energy being minimum with respect to $\bar{S}$, although it does not eliminate all reducible diagrams. That this last requirement is important is demonstrated by the fact that this simple renormalization does not yield a satisfactory solution to first order; all divergences are eliminated, even in the susceptibility, so that no Curie temperature is obtained.

As first-order diagrams we consider closed loops with attached chains (Cayley-Husimi trees). These chains may either terminate in open ends, or may have simple loops attached to their ends. This latter possibility associates with the first-order diagrams a certain number of higher-order diagrams, of course—this being a feature of any renormalization process. We choose $\bar{S}$ so that the contribution of the "end" of the chain (be it open or terminated by a loop) vanishes. The only first-order diagrams remaining then become the simple loops without side chains, and we therefore obtain the expression (121)

$$-\beta F_1' = -\beta N J_0 \bar{S}^2 + N \ln \sum_{-S}^{S} \exp(\beta L S_z) - \tfrac{1}{2} \sum_{\mathbf{q}} \ln[1 - 2\beta J(\mathbf{q}) M_2]. \quad \text{(C1)}$$

In this expression, the quantities L and M_2 are defined in terms of the $\bar{S}$, which still must be computed.

Consider a particular chain attached to some diagram. If the chain is open it contributes a spin factor $M_1(\sigma)$ to its diagram. If it carries all possible double bonds (the simplest closed loops) it contributes an additional factor of $(2\beta)^2 \sum_j J_{ij}^2 M_3 M_2$ to its diagram. If it carries all possible 3-bond loops it contributes $\frac{1}{2}(2\beta)^3 \sum_{jk} J_{ij} J_{jk} J_{ki} M_3 M_2^2$ to its diagram, the factor of $\frac{1}{2}$ coming from the possibility of interchanging the equivalent indices j and k. In fact, if we denote the contribution to $-\beta F$ of a closed cycle diagram by f_n, its contribution when joined to a chain is $(1/N) D F_n$, where $D M_2^n = n M_2^{n-1} M_3$; that is, D is our index-raising differential operator. The factor n accounts for the fact that any of the n points on the loop can be joined to the chain; and the promotion of one of the factors M_2 to M_3 corresponds to the effect of the

FIG. 7. Diagram (a) is eliminated, but diagram (b) is not eliminated, by the renormalization procedure of Appendix C.

jointure. The quantity f_n is the nth term in Eq. (119), and the sum of all possible contributions arising from loops attached to the end of the chain is

$$\begin{aligned} M_1(\sigma)-&\frac{\beta}{N}DF^{(1)} \\ &=M_1(\sigma)-\frac{1}{2N}D\sum_{\mathbf{q}}\ln[1-2\beta J(\mathbf{q})M_2(\sigma)] \\ &=\bar{S}-M_1(S_z)+\frac{1}{2N}\sum_{\mathbf{q}}\frac{2\beta J(\mathbf{q})M_3(\sigma)}{1-2\beta J(\mathbf{q})M_2} \\ &=\bar{S}-M_1(S_z)-\Gamma M_3(S_z), \end{aligned} \tag{C2}$$

where Γ was defined in Eq. (120). Setting the total contribution of the end of the chain equal to zero, we evaluate $\bar{S}$ by

$$\bar{S}=M_1(S_z)+\Gamma M_3(S_z). \tag{C3}$$

We now show easily that this choice of $\bar{S}$ minimizes F_1'. Differentiating Eq. (C1), which is identical to Eq. (121), we obtain the result given in Eq. (150), whence

$$(\partial F_1'/\partial\bar{S})_H=2NJ_0[\bar{S}-M_1(S_z)-\Gamma M_3(S_z)]=0. \tag{C4}$$

This relation also makes it particularly easy to compute the magnetization, by differentiating F_1' at constant $\bar{S}$,

$$\mathfrak{M}_1'=-\partial F_1'/\partial H=Ng\mu_0[M_1+\Gamma M_3]=Ng\mu_0\bar{S}.$$

Hence this renormalization achieves both of the desirable features: F_1' is minimum, and $\bar{S}$ is the magnetization. However, computing the susceptibility, we obtain

$$\begin{aligned} \chi_1'=\frac{1}{N}\frac{\partial\mathfrak{M}_1'}{\partial H}&=g\mu_0\partial\bar{S}/\partial H=g\mu_0(\partial/\partial H)[M_1+\Gamma M_3] \\ &=g^2\mu_0^2\beta\frac{M_2+\Gamma M_4+\Delta M_3^2}{1-2\beta J_0(M_2+\Gamma M_4+\Delta M_3^2)}. \end{aligned} \tag{C5}$$

The quantity ΔM_3^2 approaches zero as $\bar{S}$ approaches zero (as it must at the Curie temperature). If there is to be a transition, the remaining terms in the denominator must vanish as $\bar{S}$ vanishes. However, there is no solution to the equation

$$1=2\beta J_0[M_2+\Gamma M_4],$$

and hence this type of simple renormalization leads to no transition at all.

The fact that renormalization confined to the ends of chains eliminates the reducible diagram Fig. 7(a), but retains the diagram of Fig. 7(b), suggests that these diagrams should be treated in a symmetrical fashion. This is done by renormalization of all vertices in the diagrams, in Sec. 10.

APPENDIX D. INTEGRAL REPRESENTATION OF THE RENORMALIZED SEMI-INVARIANTS

In this Appendix we obtain an integral representation for the quantities $\bar{M}_r$ and $\bar{\phi}$. An examination of the properties of those quantities will show that the $\bar{M}_r$ retain all the basic properties of the original semi-invariants, and that $\bar{\phi}$ serves as the generating function of these renormalized semi-invariants.

We have previously defined [in Eqs. (162) and (163)] the quantities

$$\bar{M}_r(\beta L)=\bar{M}_r(x)=\exp(\bar{\Gamma}D_\Gamma^2)M_r(x), \qquad r=0,\,1,\,2,\,\cdots, \tag{D1}$$

and where in addition

$$\begin{aligned} \bar{M}_0=\bar{\phi}&=\exp(\bar{\Gamma}D_\Gamma^2)\phi(\beta L) \\ &=\exp(\bar{\Gamma}D_\Gamma^2)\ln\sum_{-S}^{S}\exp(\beta LS_z). \end{aligned} \tag{D2}$$

The differential operator D_Γ was defined by

$$D_\Gamma=(1/2\beta J_0)(\partial/\partial\bar{S}),\quad \bar{\Gamma}\text{ const.} \tag{D3}$$

The only detailed property of the M_r which we use is the index raising property of the differential operator:

$$D_\Gamma M_r=M_{r+1}. \tag{D4}$$

In particular it is to be observed that all these functions depend on the external field H and the parameter $\bar{S}$ only through the function $\beta L=x=\beta(2J_0\bar{S}+g\mu_0H)$. Thus we can also regard

$$D_\Gamma=(\partial/\partial x),\quad \bar{\Gamma}\text{ const.} \tag{D5}$$

The exponential $\exp(ikx)$ is an eigenfunction of any operator function of the form $\exp[a(d/dx)^r]$, where

$$\exp[a(d/dx)^r]\exp(ikx)=\exp[a(ik)^r]\exp(ikx). \tag{D6}$$

This suggests the utility of introducing the Fourier integral for the M_r,

$$M_r(x)=(2\pi)^{-\frac{1}{2}}\int_{-\infty}^{\infty}e^{-ikx}\tilde{M}_r(k)dk, \tag{D7}$$

where

$$\tilde{M}_r(k)=(2\pi)^{-\frac{1}{2}}\int_{-\infty}^{\infty}e^{ikx}M_r(x)dx. \tag{D8}$$

On substituting (D7) in Eqs. (D1) and (D2), we obtain for the transformed semi-invariants,

$$\bar{M}_r(x)=(2\pi)^{-\frac{1}{2}}\int_{-\infty}^{\infty}e^{-ikx}\exp(-\bar{\Gamma}k^2)\tilde{M}_r(k)dk. \tag{D9}$$

We regard this integral as the Fourier transform of the product of two functions:

$$\bar{M}_r(x)=(2\pi)^{-\frac{1}{2}}\int_{-\infty}^{\infty}F(k)G(k)e^{-ikx}dk, \quad \text{(D10)}$$

where

$$F(k)=\exp(-\bar{\Gamma}k^2), \quad \text{(D11)}$$

and

$$G(k)=\tilde{M}_r(k). \quad \text{(D12)}$$

The Fourier transforms of the two functions $F(k)$ and $G(k)$ are

$$f(x)=(2\pi)^{-\frac{1}{2}}\int_{-\infty}^{\infty}F(k)e^{-ikx}dx = (2\bar{\Gamma})^{-\frac{1}{2}}\exp(-x^2/4\bar{\Gamma}), \quad \text{(D13)}$$

and

$$g(x)=(2\pi)^{-\frac{1}{2}}\int_{-\infty}^{\infty}G(k)e^{-ikx}dx=M_r(x). \quad \text{(D14)}$$

The *Faltung* theorem relates the Fourier transform of the product $F(\boldsymbol{k})$ and $G(\boldsymbol{k})$ to an integral of the product of $f(y)$ and $g(x-y)$ in the form

$$(2\pi)^{-\frac{1}{2}}\int_{-\infty}^{\infty}F(k)G(k)e^{-ikx}dk = (2\pi)^{-\frac{1}{2}}\int_{-\infty}^{\infty}f(y)g(x-y)dy. \quad \text{(D15)}$$

Thus using Eqs. (D13) and (D14) for f and g, we obtain

$$\bar{M}_r(x)=(2\pi)^{-\frac{1}{2}}\int_{-\infty}^{\infty}(2\bar{\Gamma})^{-\frac{1}{2}}\exp(-y^2/4\bar{\Gamma}) \times M_r(x-y)dy. \quad \text{(D16)}$$

It is convenient to make the substitution

$$(2\bar{\Gamma})^{-\frac{1}{2}}y=u, \quad \text{(D17)}$$

whereby

$$\bar{M}_r(x)=(2\pi)^{-\frac{1}{2}}\int_{-\infty}^{\infty}\exp(-u^2/2)M_r[x-u(2\bar{\Gamma})^{\frac{1}{2}}]du. \quad \text{(D18)}$$

This is then the integral representation of $\bar{M}_r$ which we have sought. It will be observed that in the limit that the first-order effects become negligible, i.e.,

$$\bar{\Gamma}\to 0, \quad \bar{M}_r(x)\to M_r(x).$$

More explicitly, the $\bar{M}_r(x)$ are functions not only of $x=\beta L$, but also of the quantity $\bar{\Gamma}$. The differential properties of the $\bar{M}_r(x)$ are conveniently obtained by means of the partial derivatives $(\partial\bar{M}_r(x)/\partial x)_{\bar{\Gamma}}$ and $(\partial\bar{M}_r(x)/\partial\bar{\Gamma})_x$. The first of these is obtained directly by differentiating equation (D18):

$$\left(\frac{\partial\bar{M}_r(x)}{\partial x}\right)_{\bar{\Gamma}}=\int_{-\infty}^{\infty}\frac{\partial M_r[x-u(2\bar{\Gamma})^{\frac{1}{2}}]}{\partial x}\frac{1}{(2\pi)^{\frac{1}{2}}} \times\exp(-u^2/2)du=\bar{M}_{r+1}(x). \quad \text{(D.19)}$$

The derivative with respect to $\bar{\Gamma}$ can be obtained by differentiating equation (D16) directly and integrating by parts. It can also be obtained from the expression

$$\bar{M}_r=\exp(\bar{\Gamma}D_\Gamma^2)M_r=\sum_0^\infty\frac{1}{n!}\bar{\Gamma}^nM_{r+2n}(x), \quad \text{(D20)}$$

$$\frac{\partial\bar{M}_r}{\partial\bar{\Gamma}}=\sum_1^\infty\frac{1}{(n-1)!}\bar{\Gamma}^{(n-1)}M_{r+2n}(x) =\sum_0^\infty\frac{\bar{\Gamma}^n}{n!}M_{r+2+2n}(x)=\bar{M}_{r+2}(x). \quad \text{(D21)}$$

Thus all of these quantities can be generated by repeated operation of D_Γ on the generating function $\bar{M}_0=\bar{\phi}$, just as the M_r were generated from ϕ.

APPENDIX E. CALCULATION OF TOTAL DERIVATIVES OF $\bar{S}$ AND $\bar{\Gamma}$

Equations (154) and (160) for $\bar{S}$ and $\bar{\Gamma}$ are of the implicit form

$$\bar{S}=\bar{M}_1(\beta,H,\bar{S}(\beta,H),\bar{\Gamma}(\beta,H)), \quad \text{(E1)}$$

and

$$\bar{\Gamma}=W(\beta,H,\bar{S}(\beta,H),\bar{\Gamma}(\beta,H)). \quad \text{(E2)}$$

Differentiating with respect to H leads to coupled equations for $\partial\bar{S}/\partial H$ and $\partial\bar{\Gamma}/\partial H$:

$$\frac{\partial\bar{S}}{\partial H}=\frac{\partial\bar{M}_1}{\partial H}+\frac{\partial\bar{M}_1}{\partial\bar{S}}\frac{\partial\bar{S}}{\partial H}+\frac{\partial\bar{M}_1}{\partial\bar{\Gamma}}\frac{\partial\bar{\Gamma}}{\partial H}, \quad \text{(E3)}$$

and

$$\frac{\partial\bar{\Gamma}}{\partial H}=\frac{\partial W}{\partial H}+\frac{\partial W}{\partial\bar{S}}\frac{\partial\bar{S}}{\partial H}+\frac{\partial W}{\partial\bar{\Gamma}}\frac{\partial\bar{\Gamma}}{\partial H}. \quad \text{(E4)}$$

Similarly, for $\partial\bar{S}/\partial\beta$ and $\partial\bar{\Gamma}/\partial\beta$ we must solve the equations

$$\frac{\partial\bar{S}}{\partial\beta}=\frac{\partial\bar{M}_1}{\partial\beta}+\frac{\partial\bar{M}_1}{\partial\bar{S}}\frac{\partial\bar{S}}{\partial\beta}+\frac{\partial\bar{M}_1}{\partial\bar{\Gamma}}\frac{\partial\bar{\Gamma}}{\partial\beta}, \quad \text{(E5)}$$

$$\frac{\partial\bar{\Gamma}}{\partial\beta}=\frac{\partial W}{\partial\beta}+\frac{\partial W}{\partial\bar{S}}\frac{\partial\bar{S}}{\partial\beta}+\frac{\partial W}{\partial\bar{\Gamma}}\frac{\partial\bar{\Gamma}}{\partial\beta}. \quad \text{(E6)}$$

Recalling that

$$W=(2N)^{-1}\sum_q\{2\beta J(\mathbf{q})/[1-2\beta J(\mathbf{q})\bar{M}_2]\},$$

we compute the eight derivatives listed in (E3)–(E5):

$$\frac{1}{\beta g\mu_0}\frac{\partial\bar{M}_1}{\partial H}=\frac{1}{2\beta J_0}\frac{\partial\bar{M}_1}{\partial\bar{S}}=\bar{M}_2,$$

$$\frac{1}{\beta g\mu_0}\frac{\partial W}{\partial H}=\frac{1}{2\beta J_0}\frac{\partial W}{\partial\bar{S}}=\bar{\Delta}\bar{M}_3,$$

$$\frac{\partial\bar{M}_1}{\partial\bar{\Gamma}}=\bar{M}_3, \quad \frac{\partial W}{\partial\bar{\Gamma}}=\bar{\Delta}\bar{M}_4,$$

$$\frac{\partial\bar{M}_1}{\partial\beta}=L\bar{M}_2, \quad \frac{\partial W}{\partial\beta}=\beta^{-1}(\bar{\Gamma}+\bar{\Delta}\bar{M}_2)+\bar{\Delta}L\bar{M}_3.$$

Solving Eqs. (E3) and (E4) for $\partial\bar{S}/\partial H$ and $\partial\bar{\Gamma}/\partial H$ we obtain

$$\frac{\partial\bar{S}}{\partial H}=\beta g\mu_0\left[\bar{M}_2+\frac{\bar{\Delta}\bar{M}_3^2}{1-\bar{\Delta}\bar{M}_4}\right]\times\left[1-2\beta J_0\left(\bar{M}_2+\frac{\bar{\Delta}\bar{M}_3^2}{1-\bar{\Delta}\bar{M}_4}\right)\right]^{-1}, \quad \text{(E7)}$$

and

$$\frac{\partial\bar{\Gamma}}{\partial H}=\beta g\mu_0\left[\frac{\bar{\Delta}\bar{M}_3}{1-\bar{\Delta}\bar{M}_4}\right]\left[1-2\beta J_0\left(\bar{M}_2+\frac{\bar{\Delta}\bar{M}_3^2}{1-\bar{\Delta}\bar{M}_4}\right)\right]^{-1}. \quad \text{(E8)}$$

The solutions of Eqs. (E5) and (E6) in turn are

$$\frac{\partial\bar{S}}{\partial\beta}=\frac{L}{\beta g\mu_0}\frac{\partial\bar{S}}{\partial H}+\beta^{-1}\bar{M}_3(\bar{\Gamma}+\bar{\Delta}\bar{M}_2)\times[(1-2\beta J_0\bar{M}_2)(1-\bar{\Delta}\bar{M}_4)-2\beta J_0\bar{\Delta}\bar{M}_3^2]^{-1}, \quad \text{(E9)}$$

and

$$\frac{\partial\bar{\Gamma}}{\partial\beta}=\frac{\beta^{-1}\bar{\Gamma}(1-2\beta J_0\bar{M}_2)+\bar{\Delta}(L\bar{M}_3+\beta^{-1}\bar{M}_2-2J_0\bar{M}_2^2)}{(1-\bar{\Delta}\bar{M}_4)(1-2\beta J_0\bar{M}_2)-2\beta J_0\bar{\Delta}\bar{M}_3^2}. \quad \text{(E10)}$$

In addition to these total derivatives the derivatives of various higher order semi-invariants are of interest. Thus, for example,

$$\partial\bar{M}_2/\partial\beta=L\bar{M}_3+2\beta J_0\bar{M}_3\partial\bar{S}/\partial\beta+\bar{M}_4\partial\bar{\Gamma}/\partial\beta. \quad \text{(E11)}$$

APPENDIX F. BEHAVIOR OF THE SOLUTION AT THE CURIE TEMPERATURE

In this Appendix the behavior of the solution at the Curie temperature is examined and the results of Sec. 11 for the specific heat are validated. We examine the limits as the Curie temperature is approached from above and below as follows: To determine the behavior as T_c is approached from below, we take the limit $\beta\to\beta_c$ for nonzero H (and hence also nonzero $\bar{S}$), and we then take the limit $H\to 0$. To determine the behavior as T_c is approached from above, the limits are not so delicate, and we can first take H (and all odd semi-invariants including $\bar{S}$) to be zero, and then we allow β to approach β_c.

We evaluate several auxiliary quantities in order to obtain the limiting values of c_V at β_c as approached from both low- and high-temperature sides. One such quantity is

$$\lim_{H\to 0}\frac{1-2\beta_cJ_0\bar{M}_2}{\bar{M}_1^4}=\lim_{H\to 0}\frac{-2\beta_cJ_0}{4\bar{M}_1^3}\frac{(\partial\bar{M}_2/\partial H)}{(\partial\bar{M}_1/\partial H)}, \quad \text{(F1)}$$

where the last form of (F1) follows by the use of L'Hospital's rule. Differentiating, we obtain

$$\lim_{H\to 0}\frac{1-2\beta_cJ_0\bar{M}_2}{\bar{M}_1^4}=\lim_{H\to 0}\frac{-2\beta_cJ_0}{4}\left[\frac{\beta_cg\mu_0\bar{M}_3}{\bar{M}_1^3(\partial\bar{S}_1/\partial H)}+\frac{2\beta_cJ_0\bar{M}_3}{\bar{M}_1^3}+\frac{\bar{M}_4}{\bar{M}_1^3}\frac{(\partial\bar{\Gamma}/\partial H)}{(\partial\bar{S}_1/\partial H)}\right]. \quad \text{(F2)}$$

In the calculation of the susceptibility, Eq. (192), we saw that β_c corresponds to $2\beta_cJ_0\bar{M}_2=x^{-1}$. The quantity $\bar{\Delta}$ diverges as $F'(x)$ or $(x-1)^{-\frac{1}{2}}$. Using the divergence of $\bar{\Delta}$ at T_c we find, from Eq. (E7),

$$\lim_{H\to 0}\left(\frac{\partial\bar{S}_1}{\partial H}\right)_{\beta_c}=\frac{\beta_cg\mu_0\bar{M}_2}{1-2\beta_cJ_0\bar{M}_2+2\beta_cJ_0\bar{M}_3^2\bar{M}_4^{-1}} \quad \text{(F3)}$$

and from (E8),

$$\lim_{H\to 0}\left(\frac{\partial\bar{\Gamma}}{\partial H}\right)_{\beta_c}=\frac{-\beta_cg\mu_0\bar{M}_3\bar{M}_4^{-1}}{1-2\beta_cJ_0\bar{M}_2+2\beta_cJ_0\bar{M}_3^2\bar{M}_4^{-1}}. \quad \text{(F4)}$$

Inserting these results in Eq. (F2) we obtain

$$\lim_{H\to 0}\frac{1-2\beta_cJ_0\bar{M}_2}{\bar{M}_1^4}=\lim_{H\to 0}\frac{-(2\beta_cJ_0)^2}{4\bar{M}_2\bar{M}_4}\left(\frac{\bar{M}_3}{\bar{M}_1}\right)^3. \quad \text{(F5)}$$

We now examine

$$\lim_{H\to 0}\left(\frac{\bar{M}_3}{\bar{M}_1}\right)_{\beta_c}=\lim_{H\to 0}\frac{(\partial\bar{M}_3/\partial H)}{(\partial\bar{M}_1/\partial H)} \quad \text{(F6)}$$

again by use of L'Hospital's rule. This becomes, on differentiation,

$$\lim_{H\to 0}\left(\frac{\bar{M}_3}{\bar{M}_1}\right)_{\beta_c}=\lim_{H\to 0}\left[\frac{\beta_cg\mu_0\bar{M}_4}{\partial\bar{S}_1/\partial H}+2\beta_cJ_0\bar{M}_4+\bar{M}_5\frac{\partial\bar{\Gamma}}{\partial H}\left(\frac{\partial\bar{S}_1}{\partial H}\right)^{-1}\right], \quad \text{(F7)}$$

the other terms vanishing as a consequence of Eqs. (F3) and (F4). Thus Eq. (F5) becomes

$$\lim_{H\to 0}\frac{1-2\beta_cJ_0\bar{M}_2}{\bar{M}_1^4}=\frac{-(2\beta_cJ_0)^2}{4\bar{M}_2\bar{M}_4}(2\beta_cJ_0\bar{M}_4)^3=-\tfrac{1}{4}(2\beta_cJ_0)^2\frac{\bar{M}_4^2}{\bar{M}_2^4}, \quad \text{(F8)}$$

i.e., $1-2\beta_cJ_0\bar{M}_2$ goes to zero as $\bar{M}_1^4=\bar{S}_1^4$, while $\bar{\Delta}\sim(x-1)^{-\frac{1}{2}}$ diverges as $\bar{M}_1^{-2}$, or $\bar{M}_1^2\bar{\Delta}\sim\bar{M}_3^2\bar{\Delta}=$const at the Curie temperature.

Using these results we can evaluate [from (E10)]

$$\lim_{H\to 0}\left(\beta\frac{\partial\bar{\Gamma}}{\partial\beta}\right)_{\beta_c}=\frac{2\beta_cJ_0\bar{M}_3\bar{M}_1}{-2\beta_cJ_0\bar{M}_3^2}=-\frac{\bar{M}_1}{\bar{M}_3}=-\frac{1}{2\beta_cJ_0\bar{M}_4}, \quad \text{(F9)}$$

and from (E9)

$$\lim_{H\to 0}\left(\beta\frac{\partial\bar{S}}{\partial\beta}\right)_{\beta_c}=\frac{2\beta_c J_0\bar{M}_2\bar{M}_1}{2\beta_c J_0\bar{M}_3^2/\bar{M}_4}-\frac{\bar{M}_2\bar{M}_3}{2\beta_c J_0\bar{M}_3^2}=0. \quad \text{(F10)}$$

The specific heat is given by Eq. (202), with $H=0$,

$$\frac{c_V}{k}=-\frac{1}{N}\beta^2\frac{\partial E_1}{\partial\beta}=2\beta J_0(\bar{M}_1+\bar{M}_3\bar{\Gamma})\beta\frac{\partial\bar{S}_1}{\partial\beta}$$
$$+(\bar{M}_2+\bar{M}_4\bar{\Gamma})\beta\frac{\partial\bar{\Gamma}}{\partial\beta}+(2\beta J_0\bar{M}_1\bar{M}_3-\bar{M}_2)\bar{\Gamma}, \quad \text{(F11)}$$

and using the limiting values of $\beta\partial\bar{S}_1/\partial\beta$ and $\beta\partial\bar{\Gamma}/\partial\beta$ from (F9) and (F10) respectively, we obtain

$$\lim_{T\to T_c^-}\frac{c_V}{k}=(\bar{M}_2+\bar{M}_4\bar{\Gamma})\left(-\frac{1}{2\beta_c J_0\bar{M}_4}\right)-\bar{M}_2\bar{\Gamma}$$
$$=-\frac{\bar{M}_2^2}{\bar{M}_4}-2\bar{M}_2\bar{\Gamma}. \quad \text{(F12)}$$

Since all terms depending on odd semi-invariants vanish in the limit $T\to T_c^-$ and are identically zero ($H=0$) above T_c, it is clear the limit $T\to T_c^+$ will give the same value as $T\to T_c^-$, i.e., the specific heat is continuous at T_c. Thus

$$\lim_{T\to T_c^-}\frac{c_V}{k}=\lim_{T\to T_c^+}\frac{c_V}{k}=-\frac{\bar{M}_2^2}{\bar{M}_4}-2\bar{M}_2\bar{\Gamma}. \quad \text{(F13)}$$

The slopes of the specific heat curve for $T\lesssim T_c$ and $T\gtrsim T_c$ can be obtained from the approximate forms of c_V slightly above and below T_c. For $T\lesssim T_c$

$$\frac{1}{k}c_V\approx(\bar{M}_1+\bar{M}_3\bar{\Gamma})\left[\frac{2\beta J_0\bar{M}_1\bar{M}_2}{\bar{M}_3^2/\bar{M}_4}-\frac{\bar{\Gamma}}{\bar{M}_3\bar{\Delta}}-\frac{\bar{M}_2}{\bar{M}_3}\right]-\frac{\bar{M}_2^2}{\bar{M}_4}-2\bar{M}_2\bar{\Gamma} \quad \text{(F14)}$$

$$\lim_{T\to T_c^-}\frac{1}{k}\frac{\partial c_V}{\partial\beta}=\frac{\bar{\Gamma}(\partial\bar{\Delta}/\partial\beta)[(\bar{M}_1+\bar{M}_3\bar{\Gamma})]}{\bar{M}_3\bar{\Delta}^2}$$
$$\sim\frac{1}{\bar{\Delta}^2}\frac{\partial\bar{\Delta}}{\partial\beta}. \quad \text{(F15)}$$

Since, near $x=1$,

$$\partial\bar{\Delta}/\partial\beta\sim 1/(x-1)^{\frac{3}{4}}\sim 1/\bar{M}_1^6, \quad \text{(F16)}$$

while

$$\bar{\Delta}^2\sim 1/(x-1)\sim 1/\bar{M}_1^4, \quad \text{(F17)}$$

it follows that $\partial c_V/\partial\beta$ diverges as $\bar{M}_1^{-2}$. Similarly, for $T\gtrsim T_c$,

$$(1/k)c_V\sim-\bar{M}_2^2/\bar{M}_4-2\bar{M}_2\bar{\Gamma}; \quad \text{(F18)}$$

carrying out all differentiations and taking the limit $T\to T_c^+$, we find that

$$\lim_{T\to T_c^+}\frac{\partial c_V}{\partial\beta}$$

is finite. Thus the slope of the specific heat versus temperature curve is finite if $T\gtrsim T_c$ and is infinite if $T\lesssim T_c$.